Viscoelastic Behavior, Phase Equilibria, and Microdomain Morphology in Mixtures of a Block Copolymer and a Homopolymer

Chang Dae Han,* Deog Man Baek, and Jinhwan Kim[1]

Department of Chemical Engineering, Polytechnic University, Brooklyn, New York 11201

Kohtaro Kimishima and Takeji Hashimoto*

Polymer Chemistry Department, Faculty of Engineering, Kyoto University, Kyoto 606, Japan

Received September 26, 1991; Revised Manuscript Received February 14, 1992

ABSTRACT: Viscoelastic behavior, phase equilibria, and microdomain morphology in mixtures of a polystyrene-*block*-polybutadiene-*block*-polystyrene copolymer (Kraton 1102, Shell Development Co.) and a low molecular weight homopolymer were investigated. For the study, a series of nearly monodisperse polystyrenes (PS) and poly(α-methylstyrene)s (PαMS) with molecular weights ranging from 1200 to 9900 were synthesized via anionic polymerization, and each of the homopolymers was mixed with the block copolymer Kraton 1102. The mixtures were then characterized by means of the dynamic moduli and loss tangent using dynamic viscoelastic measurements. It was found that the solubility limits of PαMS in the block copolymer Kraton 1102 are greater than those of PS. Phase diagrams were constructed experimentally for mixtures of Kraton 1102 and homopolymer PαMS using the results of dynamic viscoelastic measurements (i.e., logarithmic plots of dynamic storage modulus versus dynamic loss modulus), which allowed us to determine the boundary between the mesophase and the homogeneous phase, and turbidity measurements, which allowed us to determine cloud point curves for liquid–liquid (macrophase) separation. Experimental results were compared with predictions made by the theory of Noolandi and co-workers. The morphological transition of the ordered microdomains as affected by the addition of homopolymer was investigated using small-angle X-ray scattering and transmission electron microscopy. Emphasis was placed on investigating the effects of molecular weight and concentration of added homopolymers on the dynamic viscoelastic behavior, phase equilibria, and morphological transition of ordered microdomains in mixtures of a block copolymer and a homopolymer.

1. Introduction

A better understanding of the viscoelastic behavior, phase equilibria, and morphology of ordered microdomains in mixtures of a block copolymer and a low molecular weight resin is of fundamental and practical importance. For instance, such mixtures are widely used in the preparation of formulas for pressure-sensitive and hot-melt adhesives. For such purposes, polystyrene-*block*-polybutadiene-*block*-polystyrene (SBS) and polystyrene-*block*-polyisoprene-*block*-polystyrene (SIS) copolymers are widely used. The reason for the use of triblock copolymers instead of diblock copolymers lies in that the polystyrene endblocks attached to the polydiene midblock provide the strength needed through microphase separation forming polystyrene microdomains on both ends of the polydiene midblock, thereby creating a physically cross-linked network structure at the service temperature.[2,3]

Since the block copolymer alone is not sufficient to give rise to the desired levels of adhesion and tack, one usually adds a low molecular weight resin to improve its wettability and contact strength properties. When a low molecular weight resin is added to an SBS or SIS triblock copolymer, a distinction must be made between one which associates (or is compatible) with the rubbery midblock of the block copolymer and one which associates with the endblocks (i.e., polystyrene microdomains). It has been reported that the addition of a midblock-associating resin (commonly referred to as tackifying resin) tends to soften the mixtures by decreasing the modulus of the polydiene midblock.[4-6] On the other hand, the addition of an endblock-associating resin tends to increase the modulus of the block copolymer due to the increased volume of the endblock.[6] Also reported in the literature is the observation that the molecular weight of added resin plays an important role in either increasing or decreasing the modulus of a given block copolymer.[6] Specifically, when added resin has a molecular weight above a certain critical value, it becomes incompatible with either of the blocks, forming a separate phase in the mixture. Under such circumstances, the mixture of a block copolymer and a low molecular weight resin does not function as an effective adhesive.[7] Recently, Han and co-workers[8-10] investigated the viscoelastic behavior and phase equilibria in mixtures of a block copolymer and a midblock-associating or endblock-associating resin.

Often, the midblock-associating and endblock-associating resins used in industry are not chemically simple materials, and in some cases their chemical structures have not been well identified. To enhance our understanding of the various phenomena which can occur when dealing with mixtures of a block copolymer and a homopolymer, it is highly desirable to use well-characterized homopolymers for investigating the viscoelastic behavior, phase equilibria, and morphology of ordered microdomains. Besides the practical importance briefly mentioned above, the microdomain morphology and phase equilibria in mixtures of a block copolymer and a homopolymer are scientifically a very challenging research area, and thus in recent years it has attracted the attention of polymer scientists. Some investigators[11-16] studied the microdomain morphology in mixtures of a diblock or triblock copolymer and a homopolymer using transmission electron microscopy or small-angle X-ray scattering (SAXS), and others studied phase equilibria in such mixtures, experimentally[14,17,18] and theoretically.[19-22]

In this paper we report the results of our recent study on the viscoelastic behavior, phase equilibria, and micro-

0024-9297/92/2225-3052$03.00/0

Table I
Molecular Characteristics of the Poly(α-methylstyrene)s and Polystyrenes Synthesized

sample code	M_w	M_w/M_n
(a) Poly(α-methylstyrene)		
PαMS1	1200	~1.3
PαMS3A	3000	~1.1
PαMS3B	3200	~1.3
PαMS4	4200	~1.3
PαMS6	6000	~1.1
PαMS8	8000	<1.2
(b) Polystyrene		
PS3A	3000	<1.1
PS3B	3300	<1.1
PS4	3700	<1.05
PS5	5000	<1.05
PS6	6100	<1.21
PS7	7800	<1.05
PS9	9900	<1.05

domain morphology in mixtures of an SBS block copolymer and a low molecular weight homopolymer, with emphasis on the effects of chemical structure, molecular weight, and concentration of added homopolymer. For the study we synthesized via anionic polymerization a series of low molecular weight poly(α-methylstyrene)s and polystyrenes.

2. Experimental Section

Materials. The block copolymer employed was an SBS triblock copolymer (Kraton D-1102, Shell Development Co.), which has block molecular weights 10430S–53600B–10430S. Osmometry was used to determine the number-average molecular weight ($M_n = 6.16 \times 10^4$), and gel permeation chromatography was used to determine the polydispersity ($M_w/M_n = 1.21$).[23] For brevity, this block copolymer will be referred to as K1102. A series of low molecular weight homopolymers, poly(α-methylstyrene)s (PαMS) and polystyrenes (PS), were synthesized via anionic polymerization. Reagent grade α-methylstyrene and styrene monomers were obtained from Scientific Polymer Products, Inc. The polymerization of α-methylstyrene was carried out with tetrahydrofuran (THF) as solvent at −78 °C, and the polymerization of styrene with toluene as solvent was carried out at 45 °C. The initiator used was *sec*-butyllithium. The solvent and monomers were purified by following the procedures in the literature.[24] The molecular characteristics of the PαMS and PS synthesized are summarized in Table I.

Sample Preparation. All samples were prepared by the solution-casting method. Predetermined amounts of K1102, PαMS (or PS) homopolymer, and antioxidant (Irganox 1010, Ciba-Geigy Group) were dissolved in toluene (10 wt % solid in toluene). The solution was cast onto a piece of Teflon releasing paper and allowed to evaporate at room temperature for 2 weeks. The mixture was then transferred to a vacuum oven and dried for 3 days at 30 °C. The temperature of the vacuum oven was raised gradually to 100 °C, and the mixture was dried at this temperature until no weight loss was observed, confirming the absence of solvent. Finally, the sample was annealed at 150 °C for 2 h. In the case of PαMS8, due to its high glass transition temperature (ca. 159 °C in the high molecular weight limit), K1102/PαMS8 mixtures were annealed at 170 °C for 1 h.

Measurement of Dynamic Viscoelastic Properties. A dynamic mechanical spectrometer (Rheometrics Inc.) operated in the parallel-plate mode (8-mm-diameter plates with a 2-mm gap) was used to obtain temperature scans (from −100 to +160 °C) of the dynamic storage modulus (G'), dynamic loss modulus (G''), and loss tangent (tan δ) for K1102/PαMS and K1102/PS samples at a fixed angular frequency of 10 rad/s.

Also used was a Model R16 Weissenberg rheogoniometer (Sangamo Control Inc.) in the cone-and-plate mode (25-mm-diameter plate and 4° cone angle with a 160-μm gap) to measure in the oscillatory shear mode the dynamic storage modulus (G') and dynamic loss modulus (G'') as functions of angular frequency (ω) at various temperatures. These measurements were used later to determine the phase boundary between the homogeneous state and the mesophase, following the procedure described elsewhere.[8-10] Data acquisition was accomplished with the aid of a microcomputer interfaced with the rheometer. Temperature control was satisfactory to within ±1 °C. In the oscillatory measurements a fixed strain of 0.003, which was well within the linear viscoelastic range of the materials investigated, was used. All experiments were conducted in the presence of nitrogen to preclude oxidative degradation of the samples.

Turbidity Measurements. A He–Ne laser (λ = 632.8 nm) light scattering apparatus constructed in our laboratory was used to determine the turbidity of mixtures of a block copolymer and a homopolymer. The turbidity measurements were used to construct cloud point curves in the mixtures. The apparatus was connected to a temperature programmer, which enabled us to specify the heating rate. Samples were placed between two glass plates, and optimum scattering angles chosen varied from about 5 to 10°, depending upon the sample.

Small-Angle X-ray Scattering. Small-angle X-ray scattering (SAXS) experiments were conducted with an apparatus, described in detail elsewhere,[25] which consists of a 12-kW rotating-anode X-ray generator, a graphite crystal for incident-beam monochromatization, a 1.5-m camera, and a one-dimensional position-sensitive proportional counter. The Cu Kα line (λ = 0.154 nm) was used. The SAXS profiles were corrected for absorption, air scattering, background scattering arising from thermal diffuse scattering, and slit-height and slit-width smearings.[26] The absolute SAXS intensity was obtained using the nickel-foil method.[27]

All the samples except for the K1102/PαMS8 mixture were first annealed at 150 °C for 2 h and subsequently cooled slowly to room temperature. The samples of K1102/PαMS8 mixtures were further annealed at 170 °C for 1 h before cooling slowly to room temperature. All the SAXS profiles in this paper were obtained at room temperature for about 3-h exposure to the incident X-ray beam.

Transmission Electron Microscopy. The microdomain structures were examined by transmission electron microscopy (TEM). For this purpose small pieces of as-cast films were first stained by osmium tetroxide vapor and embedded in epoxy resin. Ultrathin sections of ca. 50-nm thickness were obtained by microtoming at −100 °C with a Reichert Ultracut E low-temperature sectioning system. The ultrathin sections placed on electron microscope grids coated with poly(vinyl formal) and carbon-supporting films were further stained by exposure to osmium tetroxide vapor for a few hours. Electron microscopic observation was made with a Hitachi H-600 transmission electron microscope operated at 100 kV.

3. Results and Discussion

Viscoelastic Behavior of K1102/PαMS and K1102/PS Mixtures. Figure 1 gives temperature scans of dynamic storage modulus (G') and dynamic loss modulus (G''), and Figure 2 gives temperature scans of loss tangent (tan δ), for the block copolymer K1102 and the 70/30 K1102/PαMS1, 70/30 K1102/PαMS4, and 70/30 K1102/PαMS8 mixtures at a fixed frequency of 10 rad/s. It can be seen in Figure 1 that the block copolymer K1102 exhibits almost a constant value of G' in the plateau region, hereafter referred to as the plateau modulus, extending from about −60 to +40 °C, and that addition of PαMS increases significantly the plateau modulus of K1102. Notice further that the plateau modulus of the K1102/PαMS mixtures increases as the molecular weight of added PαMS increases. The observed increase in the plateau modulus of the K1102/PαMS mixtures suggests to us that added PαMS is solubilized in the PS microdomains in the block copolymer K1102.

In reference to Figure 2, we will regard the temperature at which tan δ goes through a maximum as the glass transition temperature (T_g). Values of T_g's as determined by the dynamic viscoelastic measurements are summarized in Table II. Notice in Figure 2 that the block copolymer

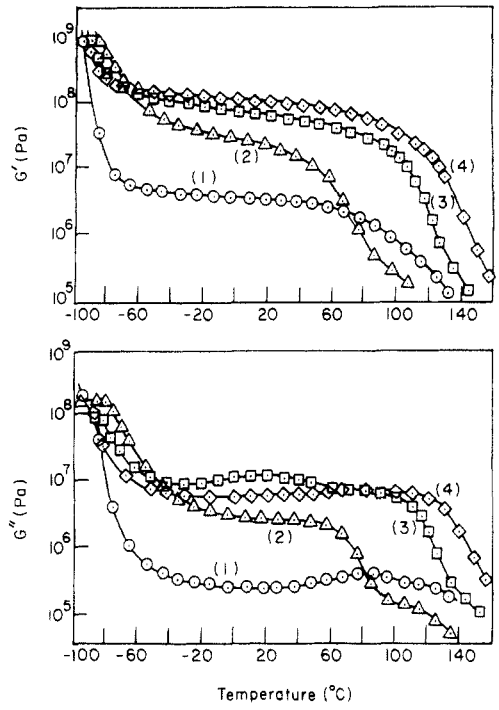

Figure 1. Temperature scans of dynamic storage modulus G' and dynamic loss modulus G'' at an angular frequency of 10 rad/s: curve 1, block copolymer K1102; curve 2, 70/30 K1102/PαMS1 mixture; curve 3, 70/30 K1102/PαMS4 mixture; curve 4, 70/30 K1102/PαMS8 mixture.

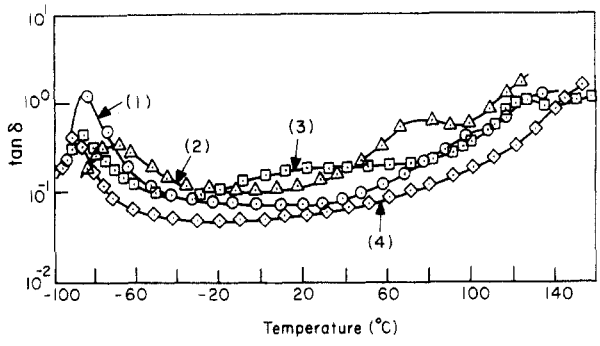

Figure 2. Temperature scans of loss tangent tan δ at an angular frequency of 10 rad/s: curve 1, block copolymer K1102; curve 2, 70/30 K1102/PαMS1 mixture; curve 3, 70/30 K1102/PαMS4 mixture; curve 4, 70/30 K1102/PαMS mixture.

K1102 exhibits a sharp peak in tan δ at about −84 °C, which represents the T_g of the polybutadiene (PB) midblock, but due to an insufficient amount of PS endblock present in the block copolymer K1102, it is difficult to discern a tan δ peak in the upper transition region, which would represent the T_g of the PS endblock. However, according to Krause et al.,[28] the T_g of homopolymer PS having the molecular weight of 10 440 is about 95 °C. Our DSC measurement showed that the glass transition temperature of the PS endblock in the block copolymer K1102, $T^b_{g,PS}$, is about 95 °C.[29]

Notice in Table II that the glass transition temperature of the PS endblock in the 70/30 K1102/PαMS1 mixture, $T^m_{g,PS}$, is 72 °C, indicating that the glass transition temperature of the PS endblock in K1102 is lowered by 23 °C with addition of homopolymer PαMS1 by 30 wt %. This makes sense in view of the fact that the T_g of homopolymer PαMS1 is lower than that of the PS endblock in K1102 and that, as shown below, about 73 wt % of added PαMS1 has been solubilized in the PS endblock of K1102. We can then conclude that PαMS1 is solubilized in both the PB midblock and the PS endblock of K1102,[30] as judged

Table II
Summary of Values of T_g for Homopolymer PαMS, Block Copolymer K1102, and K1102/PαMS Mixtures

(a) Homopolymer PαMS
T_g for PαMS1: 54 °C
T_g for PαMS4: 132 °C
T_g for PαMS7: 159 °C

(b) Block Copolymer K1102
$T^b_{g,PB}$: −84 °C
$T^b_{g,PS}$: 95 °C

(c) 70/30 K1102/PαMS1 Mixture
$T^m_{g,PB}$: −72 °C
$T^m_{g,PS}$: 72 °C

(d) 70/30 K1102/PαMS4 Mixture
$T^m_{g,PB}$: −86 °C
$T^m_{g,PS}$: 120 °C

(e) 70/30 K1102/PαMS8 Mixture
$T^m_{g,PB}$: −90 °C
$T^m_{g,PS}$: 136 °C

by the shifts of glass transition temperature toward higher temperatures in the lower transition region and also toward lower temperatures in the upper transition region.

It can be seen in Figure 2 that when the molecular weight of added PαMS is increased from 1200 to 4200 (or to 8000), it is solubilized only in the PS endblock, and not in the PB midblock of K1102,[30] as judged from the fact that no shift of the tan δ peak is observed in the lower transition region, but the tan δ peak in the upper transition region is shifted toward higher temperatures; that is, the glass transition temperature of the PS endblock in K1102 is increased with addition of homopolymers PαMS4 and PαMS8 by 30 wt %. Again, this makes sense in view of the fact that the glass transition temperatures of PαMS4 and PαMS8 are much higher than that of the PS endblock in K1102 and that, as shown below, the entire amount of added homopolymer PαMS has been solubilized in the PS endblock of K1102.

Notice in Figure 2 that a very broad tan δ peak appears in the intermediate region between the two primary tan δ peaks for the K1102/PαMS4 mixture, but not for the K1102/PαMS1 and K1102/PαMS8 mixtures. It should be remembered that the molecular weight M_w of PαMS1 is 1200, the M_w of PαMS4 is 4200, and the M_w of PαMS8 is 8000. This observation leads us to conclude that the molecular weight of added PαMS has much to do with the existence of such a broad tan δ peak appearing in the intermediate region between the two primary tan δ peaks. The physical origin(s) for the appearance of such a broad tan δ peak will be speculated on after more experimental results are presented for other mixtures.

Above, we observed that for the K1102/PαMS1 mixtures added PαMS1 was solubilized in both the PS and PB phases of the block copolymer. As a matter of fact, we can calculate the distributions, though approximate, of added PαMS1 in the PS and PB phases of the block copolymer K1102 using the following expression:[31]

$$1/T_g = w_1/T_{g1} + w_2/T_{g2} \quad (1)$$

where T_g is the glass transition temperature of the K1102/PαMS mixture, T_{g1} and T_{g2} are the glass transition temperatures of the constituent components, and w_1 and w_2 are the weight fractions of the constituent components. Our calculations indicate that about 27 wt % of added PαMS1 is solubilized in the PB phase, and the rest is solubilized in the PS phase of K1102. It should be mentioned, however, that eq 1 neglects the presence of an interface between the PS domains and the PB domains;

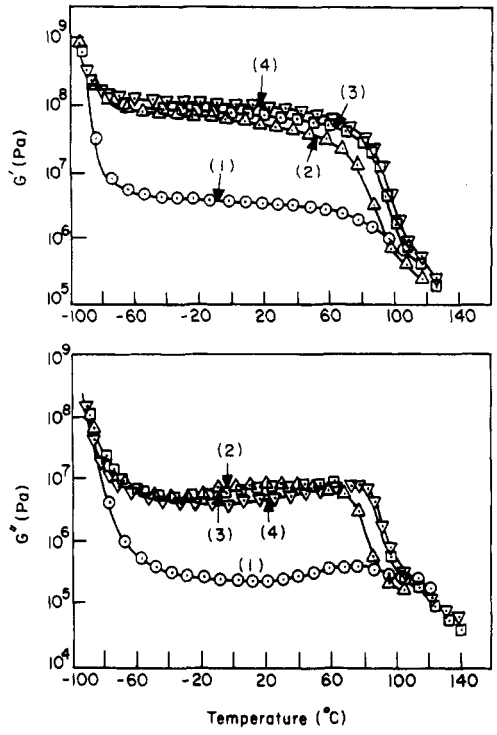

Figure 3. Temperature scans of dynamic storage modulus G' and dynamic loss modulus G'' at an angular frequency of 10 rad/s: curve 1, block copolymer K1102; curve 2, 70/30 K1102/PS4 mixture; curve 3, 70/30 K1102/PS6 mixture; curve 4, 70/30 K1102/PS9 mixture.

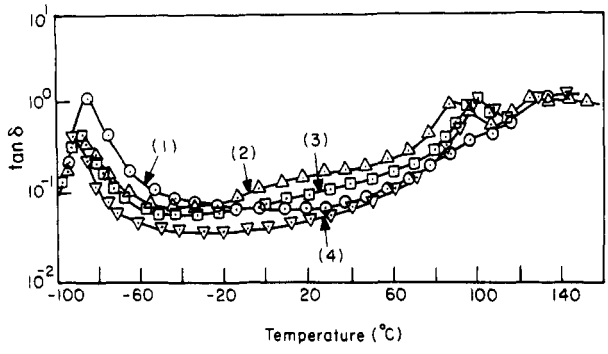

Figure 4. Temperature scans of loss tangent tan δ at an angular frequency of 10 rad/s: curve 1, block copolymer K1102; curve 2, 70/30 K1102/PS4 mixture; curve 3, 70/30 K1102/PS6 mixture; curve 4, 70/30 K1102/PS9 mixture.

thus our calculation gives only an approximate picture of the distribution of added PαMS1 in the block copolymer K1102. Nevertheless, the use of eq 1 helps us to correctly interpret the results of the dynamic viscoelastic measurements, as discussed later. The interpretation was confirmed also by analysis of the SAXS invariant.

Figure 3 gives temperature scans of G' and G'', and Figure 4 gives temperature scans of tan δ, for the block copolymer K1102 and the 70/30 K1102/PS4, 70/30 K1102/PS6, and 70/30 K1102/PS9 mixtures at a fixed angular frequency of 10 rad/s. It can be seen in Figure 3 that a very large increase in the plateau modulus appears in the 70/30 K1102/PS4 mixture, but a relatively small increase in the plateau modulus upon further increase of the molecular weight of added homopolymer PS (M_{HS}) is seen for the 70/30 K1102/PS6 and 70/30 K1102/PS9 mixtures. The observed subtle change of the plateau modulus with increasing M_{HS} may be related to changes in the size of PS microdomains and the size of segregated homopolymer PS domains. It has been reported that the size of PS microdomains may increase with increasing M_{HS}.[15] The size of segregated homopolymer PS domains may also

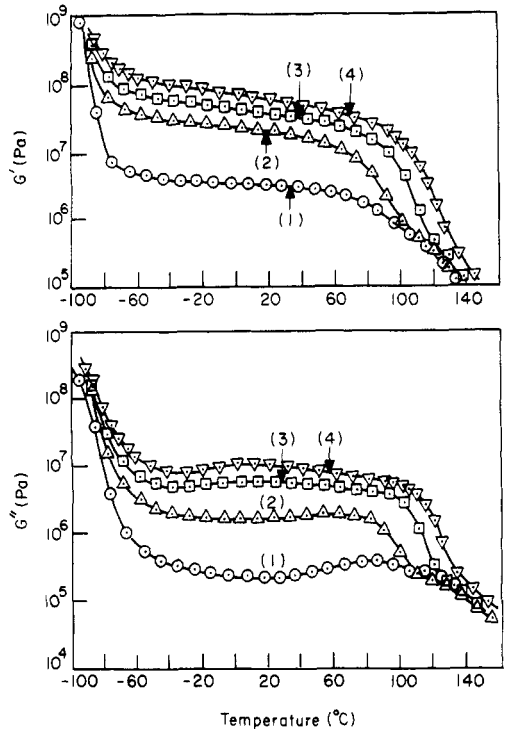

Figure 5. Temperature scans of dynamic storage modulus G' and dynamic loss modulus G'' at an angular frequency of 10 rad/s: curve 1, block copolymer K1102; curve 2, 90/10 K1102/PαMS4 mixture; curve 3, 80/20 K1102/PαMS4 mixture; curve 4, 70/30 K1102/PαMS4 mixture.

increase with increasing M_{HS}, since the thermodynamic driving force for the macrophase separation increases with increasing M_{HS}. It should be remembered that the block copolymer K1102 has cylindrical microdomains,[32] as will also be shown below. However, addition of PS4, PS6, or PS9 by 30 wt % to K1102 will change the cylindrical microdomains to lamellar microdomains. Thus we speculate that the subtle change in the plateau modulus observed in Figure 3 may also be related to an increase in orientation of the lamellar interfaces parallel to the film surface. The orientation and size of the lamellae may be closely interrelated. It should be noted that the modulus of the lamellar microdomains would be very sensitive to their orientation.

It is of interest to observe in Figure 4 that a broad tan δ peak appears in the intermediate region between the two primary tan δ peaks for the 70/30 K1102/PS4 mixture, but not for the 70/30 K1102/PS6 and 70/30 K1102/PS9 mixtures. Below, we speculate on the physical origin(s) for the appearance of such a broad tan δ peak after presenting more experimental results for other mixtures. Note further in Figure 4 that the glass transition temperature of the PB phase in the mixture (i.e., the tan δ peak in the lower transition) is not affected by the molecular weight of added homopolymer PS, implying that added homopolymer PS is selectively solubilized in the PS microdomains but not in the PB phase.

Figure 5 gives temperature scans of G' and G'', and Figure 6 gives temperature scans of tan δ, for three different concentrations of PαMS4 in the K1102/PαMS4 mixture. The following observations are worth noting in Figures 5 and 6: (1) the plateau modulus of the K1102/PαMS4 mixture increases with increasing amounts of PαMS4, suggesting that the added PαMS4 has been solubilized in the PS microdomains of the block copolymer; (2) no shift in the tan δ peak is observed in the lower transition region for all three mixtures, indicating that the molecular weight of added PαMS4 is too large for it to be solubilized in the

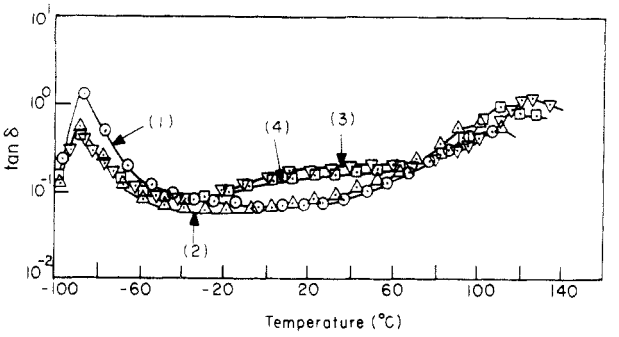

Figure 6. Temperature scans of loss tangent tan δ at an angular frequency of 10 rad/s: curve 1, block copolymer K1102; curve 2, 90/10 K1102/PαMS4 mixture; curve 3, 80/20 K1102/PαMS4 mixture; curve 4, 70/30 K1102/PαMS4 mixture.

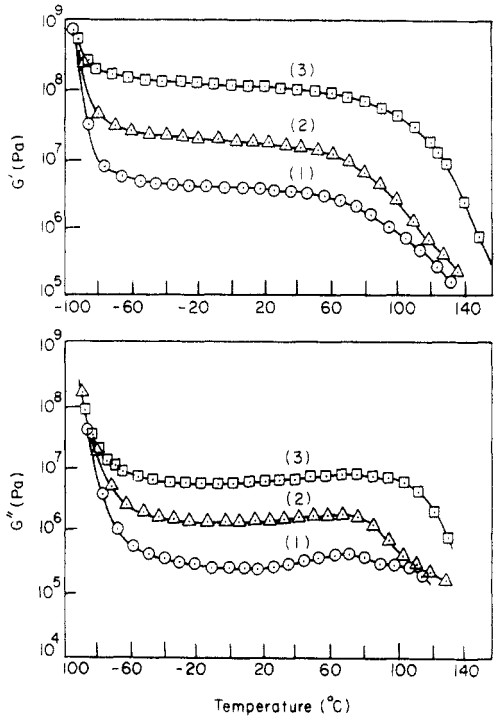

Figure 7. Temperature scans of dynamic storage modulus G' and dynamic loss modulus G'' at an angular frequency of 10 rad/s: curve 1, block copolymer K1102; curve 2, 90/10 K1102/PαMS8 mixture; curve 3, 70/30 K1102/PαMS8 mixture.

PB phase of K1102; (3) the tan δ peak in the upper transition region is shifted toward higher temperatures, indicating that added PαMS4 has been solubilized in the PS microdomains of K1102; (4) a broad tan δ peak appears in the intermediate region between the two primary tan δ peaks in the 80/20 K1102/PαMS4 and 70/30 K1102/PαMS4 mixtures, but not in the 90/10 K1102/PαMS4 mixture.

As shown below, the SAXS results indicate that a morphological change had occurred on addition of PαMS4, from K1102 being cylinders to all the blends being lamellae. Therefore we believe that the increase in the plateau modulus observed in Figure 5 is in part attributable to the morphological change which has occurred.

A question may then be raised: Why does a broad tan δ peak appear in the intermediate region between the two primary tan δ peaks as the amount of added PαMS4 in the K1102/PαMS4 mixture exceeds 10 wt %? To answer the question, let us look at the temperature scans of G' and G'' given in Figure 7, and the temperature scans of tan δ given in Figure 8, for the 90/10 K1102/PαMS8 and 70/30 K1102/PαMS8 mixtures. Remember that the molecular weights of PαMS4 and PαMS8 are 4200 and 8000,

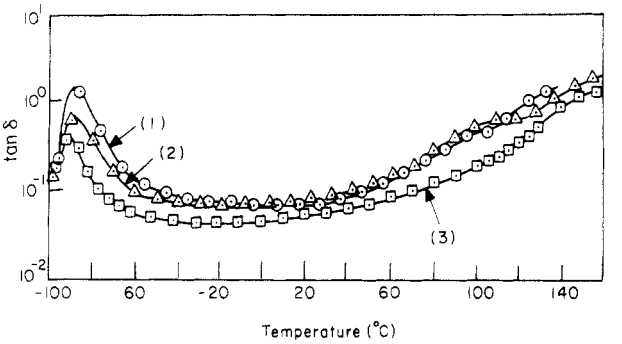

Figure 8. Temperature scans of loss tangent tan δ at an angular frequency of 10 rad/s: curve 1, block copolymer K1102; curve 2, 90/10 K1102/PαMS8 mixture; curve 3, 70/30 K1102/PαMS8 mixture.

respectively. It can be seen in Figures 7 and 8 that no broad tan δ peak appears in the intermediate region between the two primary tan δ peaks and the height of tan δ decreased as the amount of added PαMS8 increased from 10 to 30 wt %, whereas the plateau modulus of the mixture increased as the amount of added PαMS8 increased from 10 to 30 wt %. This observation rules out the possibility that macrophase separation might have taken place in the K1102/PαMS8 mixtures as the amount of added PαMS8 increased from 10 to 30 wt %. The above observation is supported by the phase diagram given below, showing that no macrophase separation takes place in the K1102/PαMS8 mixtures until the amount of added PαMS8 is increased to about 38 wt %.

At present we can only speculate that the height of a broad tan δ peak appearing in the intermediate region between the two primary tan δ peaks for certain mixtures of block copolymer K1102 with added homopolymer may be related to the thickness of an interface between the PB domain and the PS domain in the block copolymer K1102. We speculate further that the thickness of the interface may be affected by the molecular weight of added homopolymer relative to the molecular weight of the PS microdomains and, also, by the amount of added homopolymer. However, this speculation must be tested in the future by measurements of interface thickness, for instance, using solid-state NMR spectroscopy.

Phase Equilibria in K1102/PαMS Mixtures. To help interpret the results presented in Figures 1–8, we have constructed phase diagrams for mixtures of K1102 with PαMS1, PαMS4, and PαMS8, respectively. In constructing the phase diagrams, we combined the results of two independent experiments. One was dynamic viscoelastic measurements, which enabled us to determine the phase boundary between the mesophase and the homogeneous phase, and the other was turbidity measurements, which enabled us to obtain cloud point curves for the liquid–liquid (i.e., macrophase) separation between K1102 and PαMS. In the use of dynamic viscoelastic measurements to construct the phase diagrams, plots of log G' versus log G'' were prepared to determine the order–disorder transition temperature (T_r). The details of the procedures employed are described elsewhere.[8-10,32-34]

An experimental phase diagram for the K1102/PαMS1 mixture is given in Figure 9, in which H denotes a single-phase (i.e., homogeneous) mixture of disordered K1102 and PαMS1 and M_1^C and M_1^{Ch} denote mesophases, where the subscript 1 denotes the block copolymer and superscript C or Ch denotes the morphology of the mesophase, namely, C for cylindrical microdomains and Ch for irregular (chaotic) microdomains. As discussed below, the morphology of the mesophase M_1 in the K1102/PαMS1

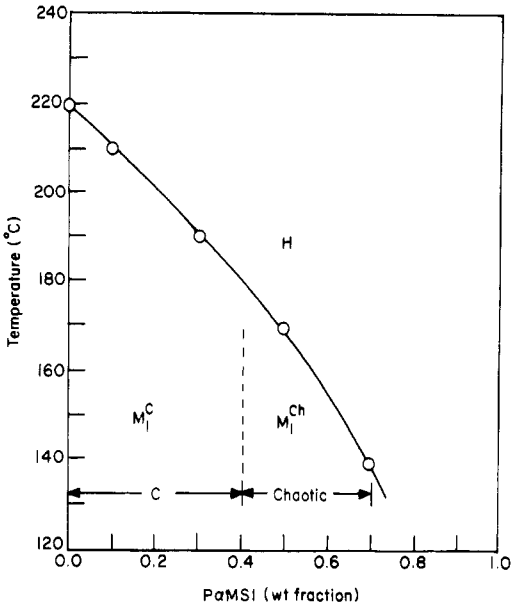

Figure 9. Experimental phase diagram for the K1102/PαMS1 mixtures, where H denotes a homogeneous mixture of K1102 and PαMS1, M_1^C denotes a mesophase having a cylindrical microdomain structure, and M_1^{Ch} denotes a mesophase having a chaotic microdomain structure. Note that the entire amount of added PαMS1 has been solubilized in the mesophase M_1.

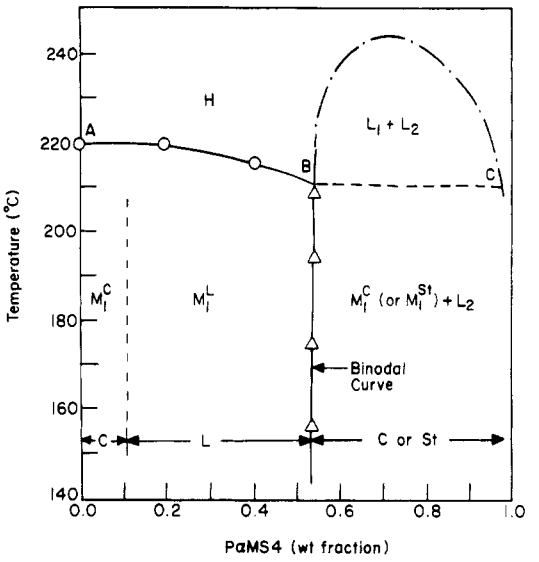

Figure 10. Experimental phase diagram for the K1102/PαMS4 mixtures, where H denotes a homogeneous mixture of K1102 and PαMS4, M_1^C denotes a mesophase having a cylindrical microdomain structure, M_1^L denotes a mesophase having a lamellar microdomain structure, M_1^{St} denotes a mesophase having a strut microdomain structure, L_1 denotes the disordered block copolymer K1102, and L_2 denotes the macrophase-separated homopolymer PαMS4. Note that the mesophase M_1 contains part of the added PαMS4 that has been solubilized.

mixtures was determined using SAXS and TEM. Notice in Figure 9 that at room temperature the morphology of the mesophase M_1 is cylinders for mixtures containing homopolymer PαMS1 up to about 40 wt % and chaotic microdomains for mixtures containing homopolymer PαMS1 from about 40 to 70 wt %. It can be seen in Figure 9 that addition of PαMS1, which has a molecular weight of 1200, steadily decreases the T_r of the mixture and that *no* macrophase separation has taken place over the entire range of compositions investigated. Note that the phase boundary between the M_1^C or M_1^{Ch} and H regions in Figure 9 was determined from dynamic viscoelastic measurements (i.e., log G' versus log G'' plots).[8-10] Figure 9 indicates that the entire amount of PαMS1 in the 70/30 K1102/PαMS1 mixture has been solubilized in the block copolymer K1102 at temperatures below 190 °C, supporting the conclusion drawn above in reference to Figure 1.

An experimental phase diagram for the K1102/PαMS4 system is given in Figure 10, in which (a) curve AB separating the mesophase (M_1^C or M_1^L) and the homogeneous phase (H) was obtained by dynamic viscoelastic measurements and the binodal curve (precisely speaking, the cloud point curve) was obtained using turbidity measurements, (b) the region denoted by (M_1^C (or M_1^{St}) + L_2) represents the mixture consisting of the mesophase (M_1^C or M_1^{St}) and the macrophage-separated PαMS4 (L_2), and (c) the region denoted by (L_1 + L_2) represents the mixture consisting of the disordered block copolymer (L_1) and the macrophase-separated PαMS4 (L_2). Note that subscript 1 denotes the block copolymer, subscript 2 denotes the added homopolymer, and superscript C, L, or St denotes the type of morphology of the mesophase (i.e., microdomains) of the block copolymer, namely, C for cylinders, L for lamellae, and St for "struts".[35] Note that the microdomains of the block copolymer inside the cloud point curve at temperatures below about 210 °C are either cylinders (C) or struts (St), which coexist with the macrophase-separated PαMS4 (L_2). The details about how the structure (C, L, or St) of microdomains was determined will be presented below. As discussed below, on the basis of SAXS and TEM investigations, at room temperature the morphology of the mesophase M_1^C inside the cloud point curve is cylinders of PB block chains and the morphology of the mesophase M_1^{St} is a three-dimensional continuous network ("strut") of PB block chains. Due to the thermal instability of the mixtures, turbidity measurements at temperatures above 230 °C were not possible, and thus the extended section (denoted by the broken curve) of the cloud point curve at temperatures above 230 °C was drawn according to theoretical predictions as presented below. It should be pointed out that the mesophase M_1^C, M_1^L, or M_1^{St} contains a portion of added PαMS4 that had been solubilized. It is of interest to observe in Figure 10 that the addition of PαMS4, which has the molecular weight of 4200, causes the T_r of the block copolymer K1102 to decrease very gradually until macrophase separation occurs. Figure 10 indicates that the entire amount of PαMS4 in the 70/30 K1102/PαMS4 mixture has been solubilized in the microdomains of the block copolymer K1102 at temperatures below about 220 °C, supporting the conclusions drawn above in reference to Figure 1.

An experimental phase diagram for the K1102/PαMS8 mixtures is given in Figure 11, in which the symbols M_1^C, M_1^L, M_1^{St}, L_1, and L_2 have the same meanings as in Figure 10. Notice in Figure 11 that the mixtures inside the cloud point curve at temperatures below about 255 °C consist of microphase-separated block copolymer having the morphology of struts (M_1^{St}) and macrophase-separated PαMS8 (L_2) and that the mixtures inside the cloud point curve at temperatures above about 255 °C consist of disordered block copolymer (L_1) and homopolymer PαMS8 (L_2). As discussed below, inside the cloud point curve at temperatures below about 255 °C the morphology of the mesophase in mixtures containing more than 65 wt % of PαMS8 was not determined. Due to the thermal instability of the mixtures, neither rheological measurements nor turbidity measurements were possible at temperatures above 240 °C, and thus the extended section (denoted by the broken curve) of curve AB and also the extended section of the cloud point curve (denoted by the broken curve) were drawn according to theoretical predictions as presented below. One notable difference in the shape of

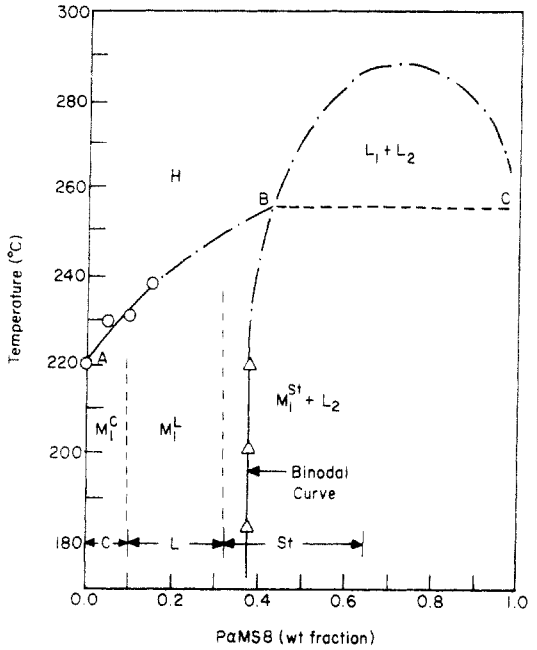

Figure 11. Experimental phase diagram for the K1102/PαMS8 mixtures, where H denotes a homogeneous mixture of K1102 and PαMS8, M_1^C denotes a mesophase having a cylindrical microdomain structure, M_1^L denotes a mesophase having a lamellar microdomain structure, M_1^{St} denotes a mesophase having a strut microdomain structure, L_1 denotes the disordered block copolymer K1102, and L_2 denotes the macrophase-separated homopolymer PαMS8. Note that the mesophase M_1 contains part of the added PαMS8 that has been solubilized.

the phase diagrams between Figures 10 and 11 is that as the molecular weight of PαMS is increased from 4200 to 8000, the addition of PαMS increased the T_r of the mixture; i.e., the slope of curve AB in Figure 11 is positive whereas the slope of curve AB in Figure 10 is negative. Notice in Figure 11, as will be discussed below on the basis of SAXS and TEM investigations, that at room temperature the morphology of the mesophase M_1^L is lamellae (denoted by L) and the morphology of the mesophase M_1^{St} is strut microdomains (denoted by St).

Using a density functional formalism on the basis of mean-field theory and employing the fourth-order expansion of the free energy of the microphase, Hong and Noolandi[21] developed a statistical thermodynamic theory, which enables one to construct phase diagrams for mixtures of a block copolymer and a homopolymer. We employed the Hong–Noolandi theory to construct phase diagrams for the K1102/PαMS1, K1102/PαMS4, and K1102/PαMS8 mixtures, and they are displayed in Figures 12–14. It should be mentioned that in predicting the phase diagrams presented in Figures 12–14, we treated the SBS triblock copolymer as an SB diblock copolymer by dividing the molecular weight of the midblock polybutadiene in half. The reason for having done this was due to the fact that the Hong–Noolandi theory is based on an AB-type diblock copolymer. In obtaining Figures 12–14 we used the expressions for the interaction energy density given in Table III and the expressions for specific volume given in Table IV. Note that the Flory–Huggins interaction parameter χ is related to the interaction energy density Λ by $\chi = \Lambda V_r/RT$, where R is the universal gas constant, T is the absolute temperature, and V_r is the reference volume. It should be mentioned that styrene was chosen as the reference component in computing values of χ for the PS/PB pair, and α-methylstyrene was chosen as the reference component in computing values of χ for the PS/PαMS and PB/PαMS pairs.

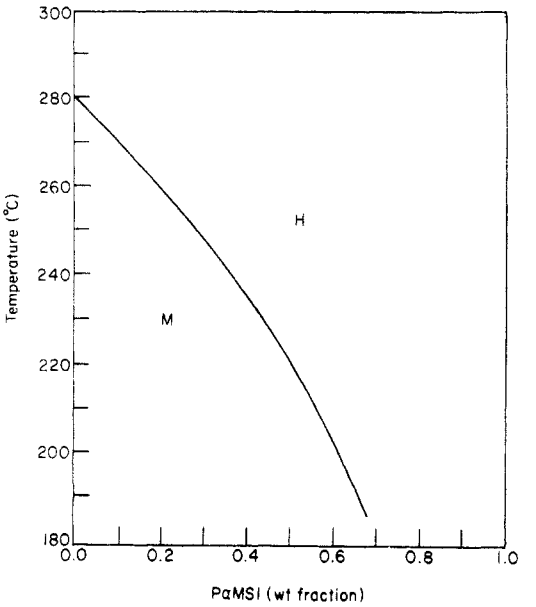

Figure 12. Predicted phase diagram for the K1102/PαMS1 mixtures, where H denotes a homogeneous mixture of K1102 and PαMS1 and M denotes a mesophase in which the entire amount of added PαMS1 has been solubilized.

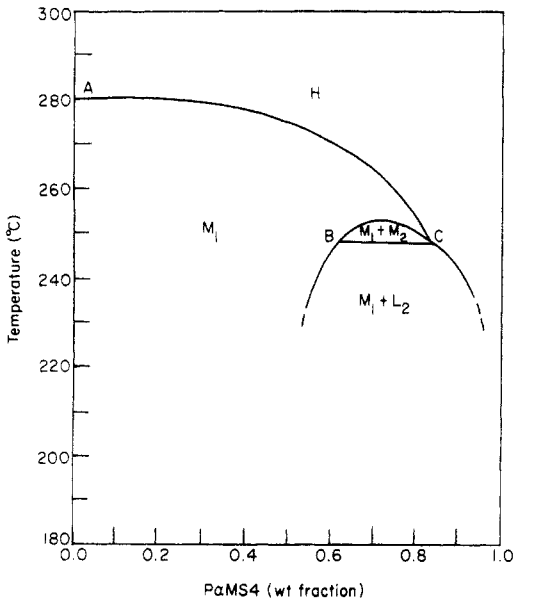

Figure 13. Predicted phase diagram for the K1102/PαMS4 mixtures, where H denotes a homogeneous mixture of K1102 and PαMS4, M_1 denotes a mesophase containing part of the added PαMS4 that has been solubilized, L_2 denotes the macrophase-separated PαMS4, and M_2 denotes a mesophase containing micellar aggregates of the block copolymer K1102 suspended in the PαMS4 medium.

It should be pointed out that the phase boundary separating the mesophase (M) and the homogeneous phase (H) in the theoretical phase diagrams (Figures 12–14) represents the spinodal temperature (T_s) for microphase separation, while it represents the order–disorder transition temperature (T_r) in the experimental phase diagrams (Figures 9–11). In view of the fact that the differences between T_s and T_r are small for pure block copolymers,[41] for the purpose of our discussion here we will assume that T_s is the same as T_r, which seems reasonable when considering the experimental uncertainties involved in determining values of T_r.

Notice in Figure 12 that the addition of PαMS1 decreases steadily the T_s of K1102, very similar to that observed experimentally (see Figure 9). It is of interest to observe

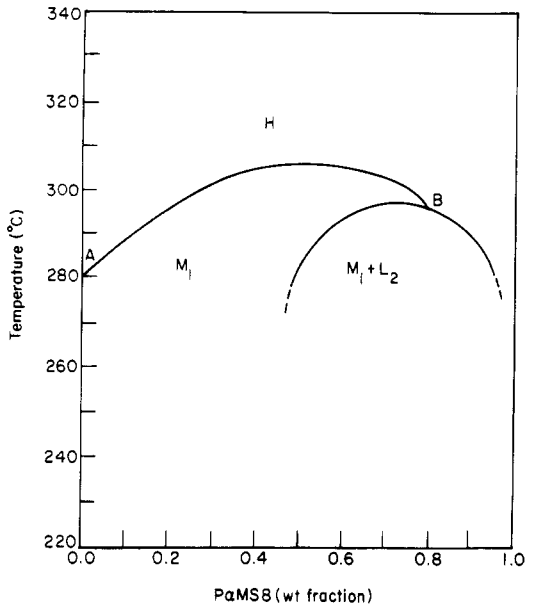

Figure 14. Predicted phase diagram for the K1102/PαMS8 mixtures, where H denotes a homogeneous mixture of K1102 and PαMS8, M_1 denotes a mesophase containing part of the added PαMS8 that has been solubilized, and L_2 denotes the macrophase-separated PαMS8.

Table III
Expressions for the Interaction Energy Density Λ for the Polymer Pairs Investigated[a]

polymer pair	interaction energy density, cal/cm³
polystyrene/polybutadiene[b,c]	$\Lambda_{PS/PB} = 1.573 - 0.0021T + 0.09\phi_{PS}$
polystyrene/poly(α-methylstyrene)[c]	$\Lambda_{PS/P\alpha MS} = 0.0608 - 0.56 \times 10^{-4}T + 0.0018\phi_{P\alpha MS}$
polybutadiene/poly(α-methylstyrene)[c]	$\Lambda_{PB/P\alpha MS} = 1.276 - 0.00183T - 0.021\phi_{PB}$

[a] T is the absolute temperature; ϕ is the volume fraction. [b] Reference 36. [c] Reference 37.

Table IV
Expressions for the Specific Volumes of the Polymers Investigated[a]

polymer	specific volume, cm³/g
polystyrene[b]	$v_{PS} = 0.9199 + 5.098 \times 10^{-4}(T - 273) + 2.354 \times 10^{-7}(T - 273)^2 + (32.46 + 0.1017(T - 273))/M_{w,PS}$
polybutadiene[c]	$v_{PB} = 1.1138 + 8.24 \times 10^{-4}(T - 273)$
poly(α-methylstyrene)[d]	$v_{P\alpha MS} = 0.87 + 5.08 \times 10^{-4}(T - 273)$

[a] T is the absolute temperature; $M_{w,PS}$ is the molecular weight of polystyrene. [b] Reference 38. [c] Reference 39. [d] Reference 40.

that the slope of the curve separating the mesophase (M) and the homogeneous phase (H) in Figure 12 is very similar to that in the experimental phase diagram (Figure 9). However, a comparison of Figure 12 with Figure 9 reveals that the values of T_s in the theoretical phase diagram are about 60 °C higher than those in the experimental phase diagram. Therefore, if the predicted value of T_s (280 °C) for the block copolymer K1102 is scaled down to 220 °C, we will obtain a reasonably good agreement between the predicted and experimental phase diagrams.

Table V gives a summary of values of $T_s/T_s°$ and $T_r/T_r°$ for K1102/PαMS mixtures, in which T_s is a theoretical spinodal point for K1102/PαMS mixtures, $T_s°$ is a theoretical spinodal point for K1102, T_r is an experimental order–disorder transition temperature for K1102/PαMS mixtures, and $T_r°$ is an experimental order–disorder transition temperature for K1102. Note that the value of $T_s°$ was determined by Leibler's theory,[41] and values of T_s were determined using the Hong–Noolandi theory.[21] It

Table V
Comparison of Predicted Values of $T_s/T_s°$ with Experimental Values of $T_r/T_r°$

material	$T_s/T_s°$	$T_r/T_r°$
90/10 K1102/PαMS1	0.965	0.955
70/30 K1102/PαMS1	0.885	0.864
50/50 K1102/PαMS1	0.784	0.773
30/70 K1102/PαMS1	0.647	0.636
80/20 K1102/PαMS4	1.000	1.000
60/40 K1102/PαMS4	0.991	0.955
90/10 K1102/PαMS8	1.032	1.045
80/20 K1102/PαMS8	1.056	1.081

is of interest to observe in Table V that the two ratios $T_s/T_s°$ and $T_r/T_r°$ are reasonably close to each other.

In Figure 13 it can be seen that curve AC meets the right side of the binodal curve, giving rise to a region denoted by (M_1 + M_2), which does not exist in the experimental phase diagram (see Figure 10). According to Roe and Zin,[17] M_2 represents a mesophase that contains micellar aggregates of the block copolymer suspended in the homopolymer medium. We already mentioned that M_1 represents a mesophase consisting of ordered microdomains of the block copolymer K1102 swollen with PαMS4. In Figure 13, we have not specified the type of morphology (cylinders, lamellae, or struts) in the mesophase M_1 (see Figures 10 and 11), because the theory assumes lamellar microdomains regardless of whether the block copolymer contains a homopolymer or not. One should bear in mind, therefore, that comparison between experimental and theoretical phase diagrams is not straightforward, since morphological transition can take place in the experimental system. For example, in reference to Figure 13, if a 30/70 K1102/PαMS4 mixture is quenched from a temperature in region H to one in region (M_1 + L_2), the resulting structure may be close to that predicted by the theoretical phase diagram. However, if the mesophase M_2 is formed during the quenching, this structure could become metastable even at a lower temperature inside the region (M_1 + L_2) and may relax extremely slowly to the equilibrium structure predicted by the phase diagram. In this case it would be very difficult to obtain experimentally the phase boundary for (M_1 + M_2) or (M_1 + L_2).

It should be mentioned that, rigorously speaking, a comparison of phase diagrams between experiment and theory is not warranted, because the theory assumes lamellar microdomains, whereas, as discussed below on the basis of SAXS and TEM investigations, for certain blend compositions the K1102/PαMS4 and K1102/PαMS8 mixtures respectively have either cylindrical microdomains or strut morphology. For the sake of argument, if curve AC in Figure 13 is scaled downward by about 60 °C, the resulting phase diagram would look very similar to the experimental phase diagram given in Figure 10. Similarly, if curve AB in Figure 14 is scaled downward by about 60 °C, the resulting phase diagram would look very similar to the experimental phase diagram given in Figure 11. However, if the discrepancies observed between the experimentally determined T_r and the theoretically predicted T_s have arisen from an inaccuracy of the values of the interaction parameters used, a downward scaling of curve AC in Figure 13 will also cause a downward scaling of curve BC. It should be mentioned that when using the Hong–Noolandi theory to construct the phase diagrams given in Figures 13 and 14, the computer programs we used did not calculate the binodal lines arbitrarily close to compositions corresponding to ϕ_H equal to 0 or 1. In our calculations, they were terminated on the right side at ϕ_H = 0.95. We believe that this is attributable to the

fact that the theory is based on a perturbation near the spinodal point; thus it would not be applicable at temperatures far away from the spinodal point.

Note that, like Leibler's theory for pure block copolymers, the Hong–Noolandi theory[21] for mixtures of a block copolymer and a homopolymer is a mean-field theory, an approximation which is rigorously valid only for an infinite molecular weight block copolymer. More recently, Fredrickson and Helfand[42] took into account a finite-sized diblock copolymer and improved the Landau-type mean-field prediction, yielding

$$(\chi N)_t = 10.495 + 41.022N^{-1/3} \quad (2)$$

for a symmetric diblock copolymer with equal block lengths ($f = 0.5$) and, also, equal Kuhn statistical lengths, with $(\chi N)_t$ referring to the location of the transition induced by composition fluctuations, Flory interaction parameter χ, and degree of polymerization N. Note that the derivation of eq 2 includes the effect of composition fluctuations on the microphase separation transition (MST), which was neglected in Leibler's final equation, $(\chi N)_t = 10.495$, although the importance of this effect was pointed out by Leibler. In view of the fact that χ is inversely proportional to temperature (see Table III), it can be seen in eq 2 that the presence of the second term $41.022N^{-1/3}$ will lower the predicted value of the transition temperature below the value based on the first term alone.

For asymmetric block copolymers having unequal block lengths ($f \neq 0.5$) and, also, unequal Kuhn statistical lengths, such as K1102 under consideration, we must use in place of eq 2 the general expression[42]

$$(\chi N)_t = (\chi N)_s - (1/2)c^2\tau^*(d\lambda)^{2/3}\tilde{N}^{-1/3} \quad (3)$$

where $(\chi N)_s$ is the value of χN at the spinodal point, $\tilde{N}$ is the reduced degree of polymerization defined by $\tilde{N} = N[(b^6/v^2)_{PS}(b^6/v^2)_{PB}]^{1/2}$ in which b is the Kuhn statistical length and v is the statistical segment volume, and c is defined by

$$c = \left[\frac{x}{3}\frac{\partial^2 F(x,f)}{\partial x^2}\right]^{1/2}_{x=x^*} \quad (4)$$

where $F(x,f)$ is defined by[41]

$$F(x,f) = g(1,x)/\{g(f,x)\,g(1-f,x) - (1/4)[g(1,x) - g(f,x) - g(1-f,x)]^2\} \quad (5)$$

in which $g(f,x)$ is the Debye function defined by

$$g(f,x) = (2/x^2)[fx + \exp(-fx) - 1] \quad (6)$$

and x is defined by

$$x = q^2Nb^2/6 = q^2/R_g^2 \quad (7)$$

where q is the magnitude of the wave vector and R_g is the radius of gyration of an ideal chain. It should be mentioned that x^* appearing in eq 4 denotes the value of x, defined by eq 7, at the spinodal point. τ^* in eq 3 is a dimensionless parameter defined by[43] $\tau^* = \tau(d\lambda)^{-2/3}\tilde{N}^{1/3}$, where τ is defined by[42] $\tau = [F(x^*,f) - 2\chi N]/c^2$. Note that τ^* is a constant (−2.0308) for lamellar microdomains, but it varies with $\tilde{N}$ for spherical and cylindrical microdomains, respectively. Note further that τ and λ appearing in eq 3 are related to Leibler's coefficients α_n and β_n,[41] and d is given by

$$d = 3x^*/2\pi \quad (8)$$

Since K1102 is an SBS triblock copolymer with $f = 0.24$, in the course of using eq 3, which was derived for an AB-type diblock copolymer, we treated the SBS triblock copolymer as an SB diblock copolymer by dividing the molecular weight of the midblock polybutadiene in half and then evaluates the parameters c, τ^*, d, λ, and $\tilde{N}$ appearing in eq 3. We obtained the following expression for K1102:

$$(\chi N)_t = 19.261 + 105.58\tilde{N}^{-1/3} \quad (9)$$

Using $N = 595$, which is based on half of the molecular weight of K1102, we calculate $\tilde{N}$ to be 2843, yielding $105.58\tilde{N}^{-1/3} = 7.452$. In carrying out numerical computations, however, we learned that the Fredrickson–Helfand theory did not predict the existence of spherical microdomains for $\tilde{N} = 2843$, confirming the observation reported earlier[42] that, owing to the nature of the Hartree approximation employed, the use of eq 3 is only valid for $\tilde{N} \geq 10^4$. Therefore, we can conclude that eq 3 is not directly applicable to predict correct values of T_r for K1102.

Recently, Burger et al.[43] considered the polydispersity effect on composition fluctuations in the MST of diblock copolymers and concluded that for a diblock copolymer having a broad molecular distribution their theory predicts the existence of spherical microdomains even when the value of $\tilde{N}$ is about 10^4. In the present study we applied the analysis of Burger et al. to the block copolymer K1102 having a polydispersity index (M_w/M_n) of 1.21 and $\tilde{N} = 2843$. We found that the existence of spherical microdomains was *not* predicted, suggesting that the values of $M_w/M_n = 1.21$ and $\tilde{N} = 2843$ for K1102 were not sufficiently large. Note that since the values of $(\chi N)_{s,poly}$ for polydisperse block copolymers are smaller than the values of $(\chi N)_{s,mono}$ for monodisperse block copolymers, the inclusion of the polydispersity effect will predict higher values of T_r than Leibler's theory, which considers monodisperse block copolymers. Thus, the inclusion of the polydispersity effect counterbalances the contribution of composition fluctuations to $(\chi N)_t$, insofar as predicting the order–disorder transition temperature of a block copolymer is concerned.

To illustrate the point, let us apply the analysis of Burger et al.[43] to the block copolymer K1102. Using $M_w/M_n = 1.21$ and $\tilde{N} = 2843$ ($f = 0.239$), we obtain

$$(\chi N)_t = (\chi N)_{s,poly} + (\chi N)_{t,fluct} = 16.285 + 6.015 \quad (10)$$

where the first term represents the contribution from the polydispersity effect and the second term represents the contribution from composition fluctuations. Notice that the value of $(\chi N)_t$ is 22.30 from eq 10, the value of $(\chi N)_t$ is 26.713 from eq 9, and Leibler's theory predicts $(\chi N)_t = 18.639$ for a transition from the disordered phase to the spherical microdomain structure. Thus we observe that the value of $(\chi N)_t$ which includes composition fluctuations is larger than the value predicted by Leibler's theory, thus lowering the value of T_r predicted by Leibler's theory, and that the value of $(\chi N)_t$ which includes both the polydispersity effect and composition fluctuations is smaller than the value of $(\chi N)_t$ predicted by the Fredrickson–Helfand theory, thus raising the value of T_r predicted by the Fredrickson–Helfand theory. We emphasize once again that the above analysis is merely to show the trend as to how the inclusion of composition fluctuations and/or the polydispersity effect modifies Leibler's theory.

It seems appropriate to mention at this juncture that the Helfand–Wasserman theory[44] predicts the T_r of 230 °C for the block copolymer K1102,[45] which is reasonably close to the measured value, 220 °C. However, in its present form the Helfand–Wasserman theory cannot be

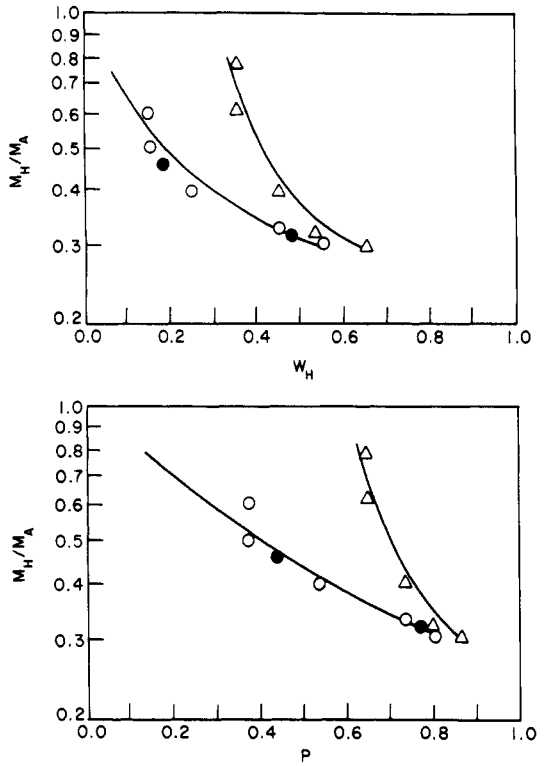

Figure 15. Solubility of homopolymers PαMS and PS in the block copolymer K1102, in which open circles represent solubility limits of homopolymer PS in the block copolymer K1102 and open triangles represent solubility limits of homopolymer PαMS in the block copolymer K1102. M_H is the molecular weight of added homopolymer, M_A is the molecular weight of the polystyrene block in K1102, W_H is the weight fraction of added homopolymer in the block copolymer/homopolymer mixture, and P is the weight fraction of homopolymer solubilized in the PS microdomains of K1102. Filled circles represent data taken from ref 17.

used to predict the T_r for mixtures of a block copolymer and a homopolymer.

Solubility Limits of PαMS and PS in K1102. We conducted experiments to determine solubility limits of homopolymers PS and PαMS in K1102. For this, we used several grades of homopolymers PS and PαMS. (See Table I for the molecular weights of the homopolymers used.)

Figure 15 gives a summary of the experimental results for investigating solubility limits determined at 50 °C. In obtaining the experimental results presented in Figure 15, we varied the concentration of homopolymer with an interval of 10 wt % and determined the turbidity, via light scattering, of mixtures of K1102 and homopolymer (PS or PαMS). Therefore the data points (i.e., the phase boundary) in Figure 15 should not be construed as exact values. The solvent effect and vitrification effect during the solution-casting process will also affect the diagram. In Figure 15 M_H denotes the molecular weight of added homopolymer (PS or PαMS), M_A denotes the molecular weight of block A (PS block in the present study) in K1102, W_H is the weight fraction of the homopolymer (PS or PαMS) in the homopolymer/block copolymer mixture, and P is defined by $H/(H + A)$, where H is the amount of homopolymer PS (or PαMS) solubilized in the PS endblock and A is the amount of PS endblock in the pure block copolymer K1102 used. The solid curves in Figure 15 were drawn through the data points. Also plotted in Figure 15 are data (denoted by a filled circle) of Roe and Zin,[17] who added homopolymer polystyrenes having molecular weights of 2400 and 3500 respectively to an SB diblock copolymer having block molecular weights of M_{PS} = 7560 and M_{PB} = 20440. It should be mentioned that we found that the hompolymer PS with a molecular weight of 2500 was soluble in the block copolymer K1102 at all concentrations; i.e., the homopolymer PS becomes soluble in the block copolymer K1102 at all concentrations when the value of M_H/M_A is below about 0.3.

Table VI
Summary of Values of the Interaction Parameter α_{12} for K1102/PαMS and K1102/PS Pairs

T, °C	$\alpha_{K1102/P\alpha MS} \times 10^4$	$\alpha_{K1102/PS} \times 10^4$
100	4.31	6.18
150	3.20	4.73
200	2.32	3.58
250	1.61	2.66

It can be seen in Figure 15 that for an equal molecular weight of added homopolymer, a greater amount of PαMS, as compared to PS, can be solubilized in K1102. At first glance this may seem somewhat strange. However, this can be explained by a recent thermodynamic theory.[46-48] The essence of the theory is as follows: when a *random* copolymer AB is mixed with a homopolymer H, the Flory–Huggins interaction parameter χ_{12} for binary mixtures of the copolymer and the homopolymer can be expressed as

$$\chi_{12} = f\chi_{AH} + (1-f)\chi_{BH} - f(1-f)\chi_{AB} \qquad (11)$$

where f is the volume fraction of component B in the copolymer, χ_{AH} is the interaction parameter for component A in the copolymer and homopolymer H, χ_{BH} is the interaction parameter for component B in the copolymer and homopolymer H, and χ_{AB} is the interaction parameter for component A and component B of the copolymer. It should be pointed out that the mean-field theory based upon the random phase approximation (RPA) predicts that thermodynamic instability at $q = 0$ (q being the magnitude of the wave vector $\mathbf{q}$ of a particular Fourier mode of the concentration fluctuations) occurs at $\chi_{12} = \chi_s$ even for the mixtures of AB-type diblock copolymer and homopolymer,[49,50] where χ_{12} is given by eq 11 and χ_s is the interaction parameter χ_{12} at the spinodal point

$$\chi_s = \frac{1}{2}\left[\frac{1}{N_1\phi_1} + \frac{1}{N_2(1-\phi_1)}\right] \qquad (12)$$

where N_1 and N_2 are the degrees of polymerization for polymers 1 and 2, respectively, and ϕ_1 is the volume fraction of polymer 1. Therefore, in the context of the mean-field approximation, eq 11 should also be applicable to the mixtures of the block copolymer K1102 and homopolymer PαMS (or homopolymer PS) investigated in this study.

Table VI gives a summary of the values of the interaction parameter α_{12}, calculated with eq 11, for K1102/PαMS and K1102/PS pairs, where $\alpha_{12} = \Lambda_{12}/RT = \chi_{12}V_r$, V_r being the molecular volume of the reference component. It should be mentioned that in obtaining the values of α_{12} given in Table VI, we used expressions for the interaction energy density Λ_{12} given in Table III, neglecting the concentration-dependent term. It can be seen in Table VI that the values of α_{12} for the K1102/PαMS pair are smaller than the values of α_{12} for the K1102/PS pair. This is attributed to the fact that $\Lambda_{PS/P\alpha MS} \ll \Lambda_{P\alpha MS/PB} < \Lambda_{PS/PB}$. This now explains why the macrophase separation between K1102 and PαMS is suppressed compared with that between K1102 and PS and hence why a greater amount of homopolymer PαMS, as compared to homopolymer PS, is solubilized in the block copolymer K1102.

Morphology of Ordered Microdomains in K1102/PαMS Mixtures. In the present study, SAXS and TEM were used to investigate the morphology of ordered microdomains as affected by the addition of homopolymer

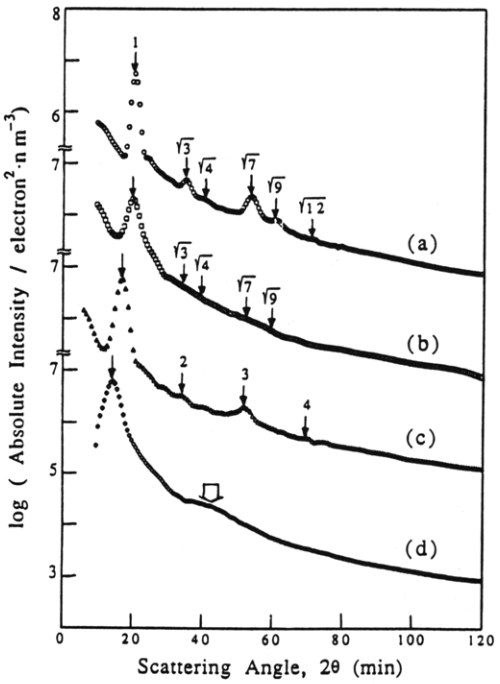

Figure 16. SAXS profiles taken at 25 °C for (a) block copolymer K1102, (b) 70/30 K1102/PαMS1 mixture, (c) 70/30 K1102/PαMS4 mixture, and (d) 70/30 K1102/PαMS8 mixture.

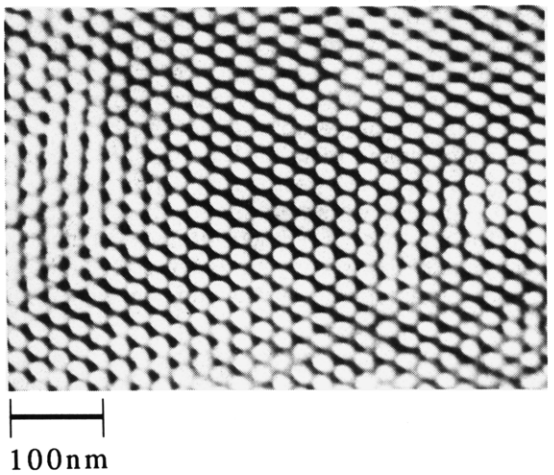

Figure 17. Transmission electron micrograph obtained on ultrathin sections stained by osmium tetroxide for the block copolymer K1102, showing the morphology at 25 °C.

PαMS. For the study, the same PαMS's as those used in the dynamic viscoelastic measurements, the results of which are presented in Figures 1–8, were used.

Figure 16 gives SAXS profiles for (a) the block copolymer K1102, (b) the 70/30 K1102/PαMS1 mixture, (c) the 70/30 K1102/PαMS4 mixture, and (d) the 70/30 K1102/PαMS8 mixture. Note in Figure 16 that the scattering angle 2θ is related to the magnitudes of the scattering vector defined by

$$s = (2 \sin \theta)\lambda \tag{13}$$

where λ is the wavelength of the X-rays in the medium. The SAXS profiles in Figure 16 indicate that the block copolymer K1102 has hexagonally packed cylindrical microdomains, as judged from the positions of higher order scattering maxima at the scattering vectors s of 1, $\sqrt{3}$, $\sqrt{4}$, $\sqrt{7}$, and $\sqrt{9}$ relative to that for the first-order scattering maximum. Figure 17 gives a TEM micrograph for the block copolymer K1102, confirming the observation made by SAXS.

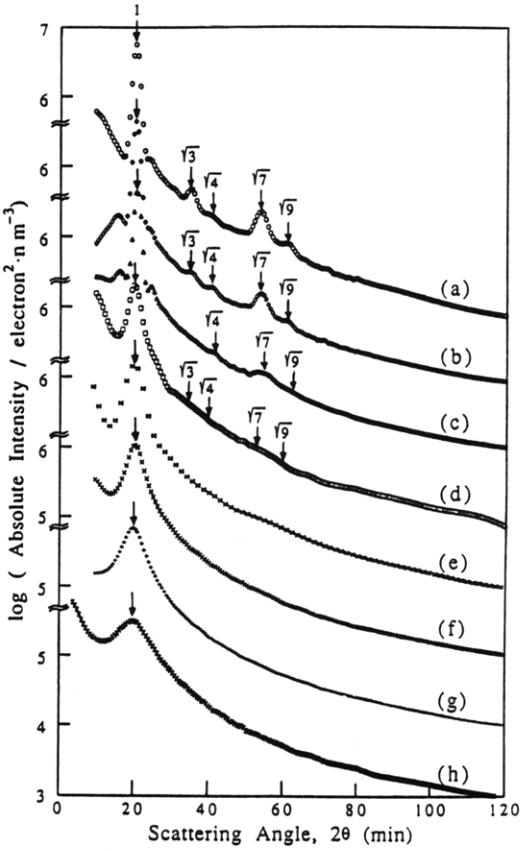

Figure 18. SAXS profiles taken at 25 °C for (a) block copolymer K1102, (b) 90/10 K1102/PαMS1 mixture, (c) 80/20 K1102/PαMS1 mixture, (d) 70/30 K1102/PαMS1 mixture, (e) 60/40 K1102/PαMS1 mixture, (f) 50/50 K1102/PαMS1 mixture, (g) 40/60 K1102/PαMS1 mixture, and (h) 30/70 K1102/PαMS1 mixture.

It is of interest to observe in Figure 16 that the 70/30 K1102/PαMS1 mixture may also have cylindrical microdomains, though the characteristic higher order peaks appear to be less clear than those for K1102. On the other hand, the 70/30 K1102/PαMS4 mixture has a lamellar microdomain structure with alternating layers of polystyrene and polybutadiene, as judged from the positions of higher order scattering maxima at integer multiples of s of the first-order scattering maximum. In other words, the addition of PαMS4 by 30 wt % has changed the morphology of ordered microdomains in the block copolymer K1102 from cylinders to lamellae, whereas addition of PαMS1 by 30 wt % has not. The observed transition in microdomain morphology of K1102 from cylinders to lamellae can be understood when we consider that the total amount of endblock in the mixture would become about 50 wt % if the entire amount (30 wt %) of added homopolymer PαMS is assumed to have been solubilized in the cylindrical microdomains of the PS endblock. According to the literature,[51-57] an SBS block copolymer having 50 wt % PS endblock has lamellar microdomain structure. This then raises an interesting question as to why the microdomain morphology of the block copolymer did not change when PαMS1 by 30 wt % was added.

The answer to this question lies in that, as pointed out above when discussing the dynamic viscoelastic measurements, only part (ca. 73 wt %) of the added PαMS1 has been solubilized in the cylindrical microdomains of PS in the block copolymer K1102, and the rest (ca. 27 wt %) has been solubilized in the PB phase. Consequently, the 70/30 K1102/PαMS1 mixture contains about 41.5% wt % PS endblock including the PαMS1 solubilized in the PS microdomains. According to the literature,[51-57] an SBS

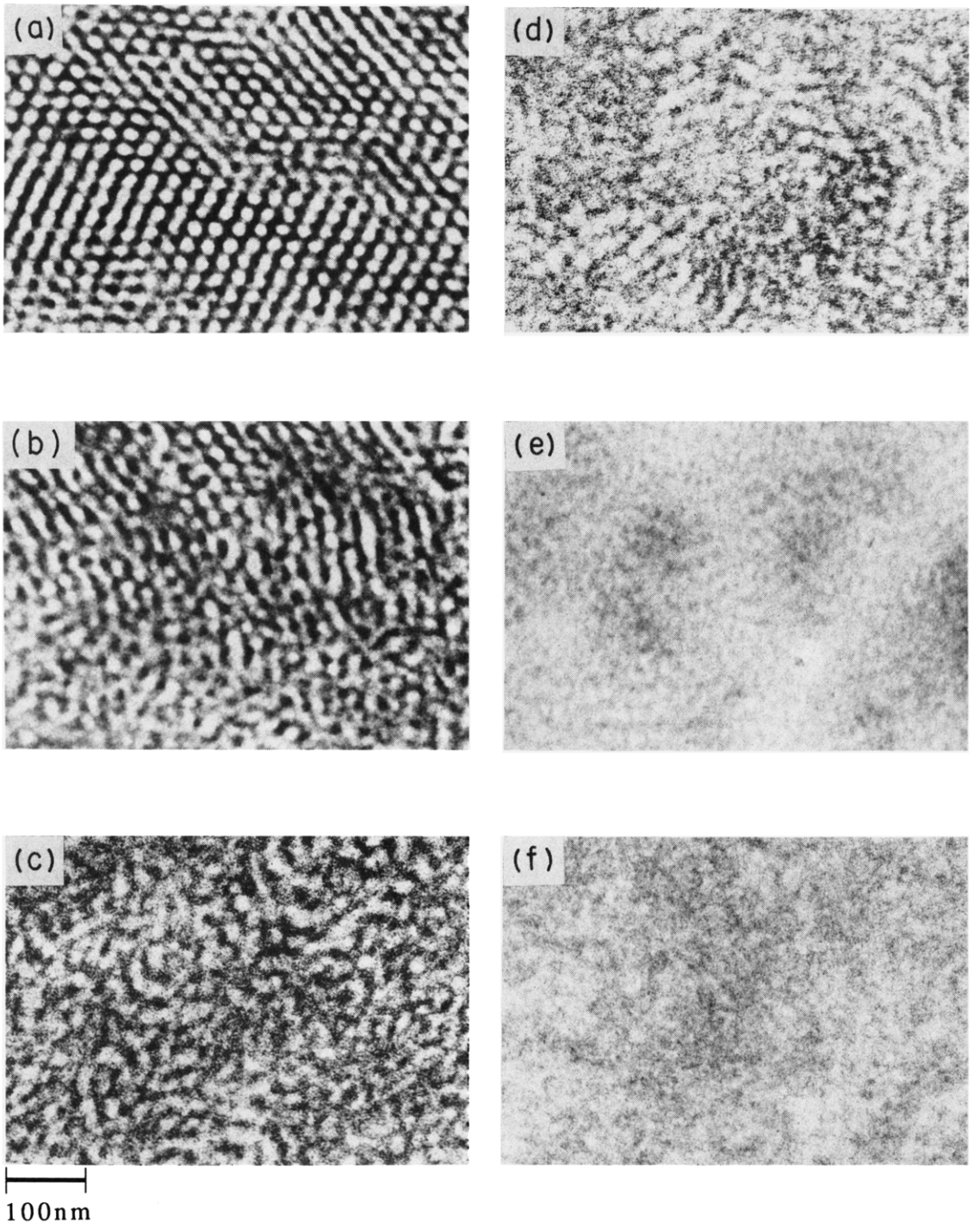

Figure 19. Transmission electron micrographs obtained on ultrathin sections stained by osmium tetroxide for (a) 90/10 K1102/PαMS1 mixture, (b) 80/20 K1102/PαMS1 mixture, (c) 70/30 K1102/PαMS1 mixture, (d) 60/40 K1102/PαMS1 mixture, (e) 50/50 K1102/PαMS1 mixture, and (f) 30/70 K1102/PαMS1 mixture, showing the morphologies at 25 °C.

block copolymer having 41.5 wt % (37.0 vol %) PS end-block (i.e., 70/30 K1102/PαMS1 mixture) has cylindrical microdomain structure.

In reference to Figure 16, the SAXS profile for the 70/30 K1102/PαMS8 mixture (curve d) is quite different from those for the hexagonally packed cylinders (curve a) and the lamellae (curve c). The TEM micrograph indicates that this is due to the scattering from a three-dimensionally interconnected network-type microdomain morphology. The 3D network structure, which is referred to as the "strut" morphology,[35] will further be elaborated on below. In Figure 16, the first-order maximum marked by a thin arrow reflects the periodicity of the 3D network, while the broad maximum marked by a thick arrow is believed to reflect the maximum arising from the uniformity in the cross-section of the network.[58]

Figure 18 gives SAXS profiles for K1102/PαMS1 mixtures containing varying amounts of PαMS1. It should be noted that (a) the turbidity experiments indicate the solubilization of PαMS1 into the K1102 phase (i.e., no macrophase separation), at least up to 70 wt % (see Figure 15a), and (b) the rheological experiments indicate further the mixtures being in the ordered state (see Figure 9). Notice in Figure 18 that the microdomain morphology remains as cylinders until the amount of added PαMS1 was increased to 30 wt %, though regularity in the hexagonal packing is progressively destroyed with increasing amount of PαMS1. As the amount of PαMS1

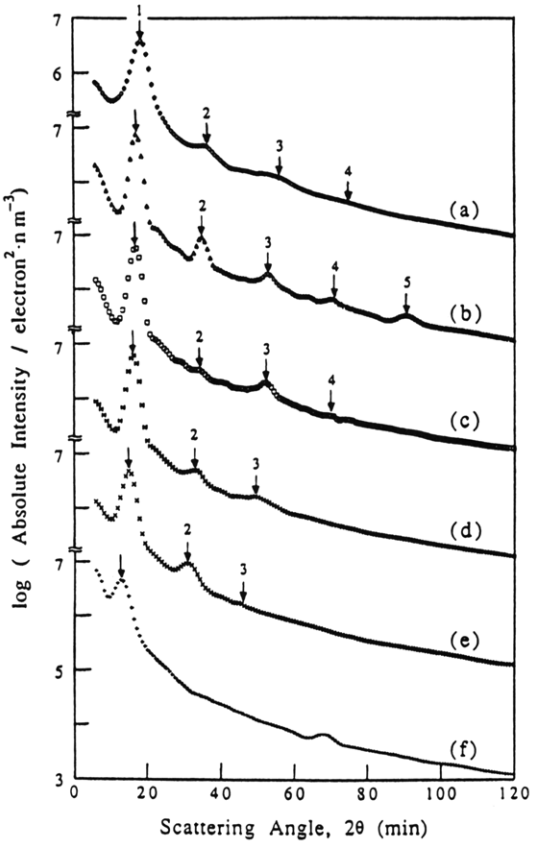

Figure 20. SAXS profiles taken at 25 °C for (a) 90/10 K1102/PαMS4 mixture, (b) 80/20 K1102/PαMS4 mixture, (c) 70/30 K1102/PαMS4 mixture, (d) 60/40 K1102/PαMS4 mixture, (e) 50/50 K1102/PαMS4 mixture, and (f) 40/60 K1102/PαMS4 mixture.

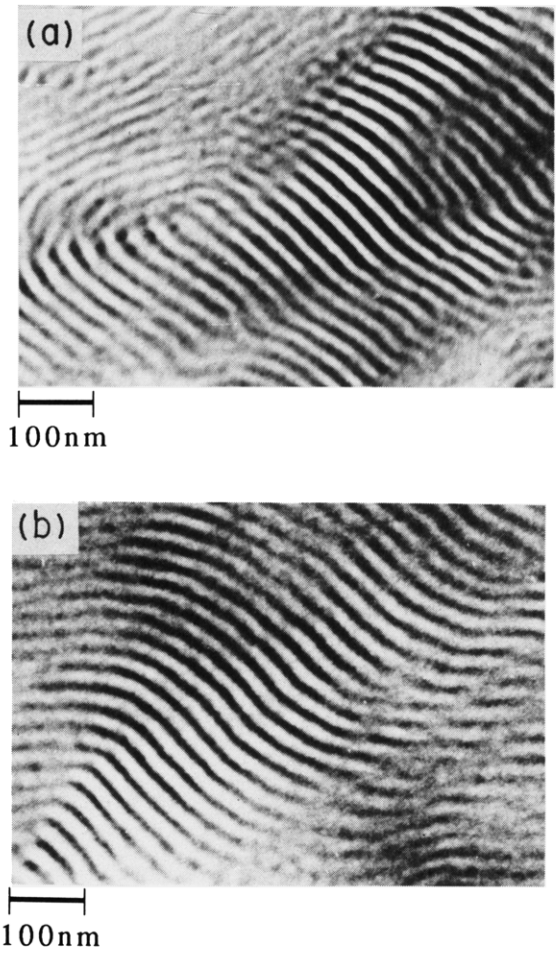

Figure 21. Transmission electron micrographs obtained on ultrathin sections stained by osmium tetroxide for (a) 80/20 K1102/PαMS4 mixture and (b) 60/40 K1102/PαMS4 mixture, showing the morphologies at 25 °C.

was increased further, the SAXS profiles look different. As reported in the literature,[59] phase inversion might occur when a sufficient amount of a homopolymer is added to a block copolymer and if the homopolymer is selectively solubilized in one type of the domains (e.g., PS domain). However, no discernible higher order scattering maxima can be observed in the SAXS profiles given in Figure 18 for the K1102/PαMS1 mixtures having more than 40 wt % PαMS1. Thus the PαMS1 which is solubilized into the microdomains tends to destroy the long-range order of the cylindrical microdomains. The SAXS data, together with rheological and light scattering data, imply that the mixture having more than 40 wt % of PαMS1 may be in the ordered state with distorted or chaotic microdomains. Figure 19 gives TEM micrographs for the K1102/PαMS1 mixtures, showing that the microdomain morphology changes with increasing amount of added PαMS1. Indeed, for mixtures containing more than 40 wt % PαMS1, no discernible cylindrical or lamellar microdomains can be observed, and the domains are substantially distorted and chaotic as shown in Figure 19.

Figure 20 gives SAXS profiles for the K1102/PαMS4 mixtures with varying amounts of PαMS4. It can be seen in Figure 20 that the microdomain morphology in the mixture shows lamellae, indicating that a morphological transition in K1102 occurred from cylinders to lamellae, until the amount of added PαMS4 reached 50 wt %, and then the SAXS profiles look quite different as the amount of PαMS4 was increased further. This observation should be closely related to the macrophase separation observed by turbidity measurement (see Figure 10) and as will be shown below by TEM micrographs.

Figure 21 gives TEM micrographs for the 80/20 and 60/40 K1102/PαMS4 mixtures, and Figure 22 gives TEM micrographs for the 40/60 K1102/PαMS4 mixture, indicating clearly that the microdomain structure is lamellar up to about 50 wt % of PαMS4 and that the 40/60 K1102/PαMS4 mixture underwent macrophase separation. This observation is corroborated by the phase diagram given in Figure 10. The large domains (white area) in Figure 22a are obviously the phase-separated PαMS4 domains, and the matrix morphology is clearly seen in the enlarged TEM micrograph shown in Figure 22b. If we assume that the entire amount (60 wt %) of added PαMS4 has been solubilized in the PS phase of K1102, the resulting 40/60 K1102/PαMS4 mixture would have about 71 wt % PS phase and the rest the PB phase. Under this circumstance, according to the literature,[53-57] the morphology of ordered microdomains would be cylinders of PB suspended in the continuous phase. In fact, we can observe in Figure 22b that the matrix morphology comprises PB cylinders or interconnected PB network (i.e., the strut morphology).

Figure 23 gives SAXS profiles for the K1102/PαMS8 mixtures with varying amounts of PαMS8, indicating that the microdomains in the mixtures have lamellar structure, at least up to 20 wt % of added PαMS8, which was confirmed by TEM, although micrographs are not shown here. When the amount of added homopolymer PαMS8 exceeds about 30 wt %, as can be seen in curves c–f of Figure 23, the microdomain morphologies of K1102/PαMS8 mixtures are no longer lamellae. Note that the results of turbidity measurement shown in Figure 11

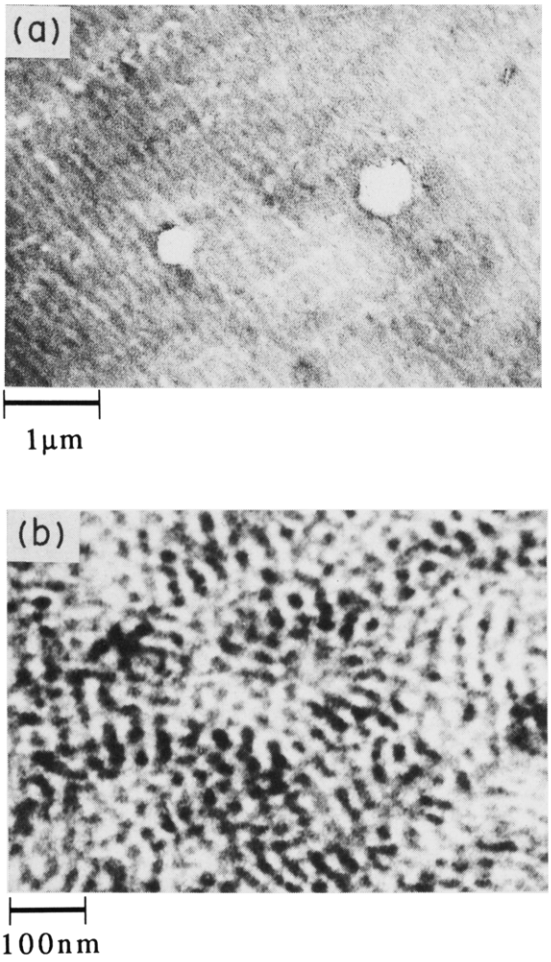

Figure 22. Transmission electron micrographs obtained on ultrathin sections stained by osmium tetroxide for the 40/60 K1102/PαMS4 mixture: (a) low magnification and (b) high magnification, showing the morphologies at 25 °C.

indicate that the mixtures having homopolymer PαMS8 greater than 40 wt % undergo macrophase separation, which was confirmed by TEM.

Figure 24 gives TEM micrographs for the 50/50 K1102/PαMS8 mixture, showing evidence of macrophase separation; specifically, the micrograph with a low magnification (Figure 24a) shows domains of macrophase-separated PαMS8 phase (white area) having sizes of about a few microns and the matrix phase (dark area) consisting of K1102 and solubilized homopolymer PαMS8. The enlarged micrographs (Figure 24b,c) clearly indicate that the matrix phase is composed of bicontinuous strut morphology, i.e., 3D network of PB microdomains in the matrix of PS and solubilized PαMS8. The micrograph given in Figure 24c highlights the fact that the morphology of the matrix phase is quite uniformly composed of struts. We belive that this strut morphology gave rise to the typical SAXS profiles, shown in curves c–f of Figure 23, in which the relatively sharp first-order peak (indicated by a thin arrow) reflects the spacing between the neighboring networks and the relatively broad second-order peak (indicated by a thick arrow) reflects the intranetwork interference peak associated with the uniformity of the cross-section of the network.[58] It is of interest to note that the spacing and the cross-section of the network increase with increasing amount of added homopolymer PαMS8.

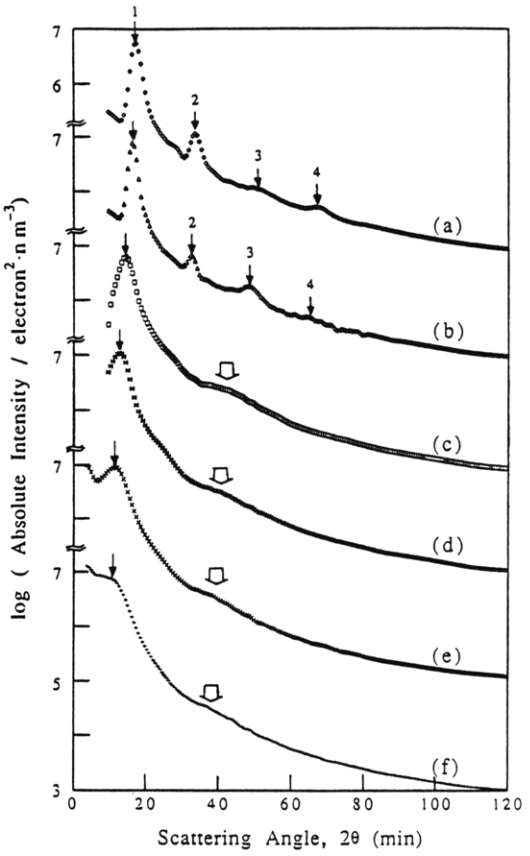

Figure 23. SAXS profiles taken at 25 °C for (a) 90/10 K1102/PαMS8 mixture, (b) 80/20 K1102/PαMS8 mixture, (c) 70/30 K1102/PαMS8 mixture, (d) 60/40 K1102/PαMS8 mixture, (e) 50/50 K1102/PαMS8 mixture, and (f) 40/60 K1102/PαMS8 mixture.

4. Concluding Remarks

We have shown in this paper that the addition of an endblock-associating homopolymer to an ABA-type block copolymer increases the dynamic storage modulus (and plateau modulus) of the block copolymer and that the critical concentration of added homopolymer at which macrophase separation takes place (i.e., solubility limits) depends on the molecular weight of added homopolymer for a given block copolymer. Our experimental results show that homopolymer PαMS has greater solubility limits in the SBS triblock copolymer K1102 than homopolymer PS, suggesting that homopolymer PαMS is more effective in increasing the plateau modulus of K1102 than homopolymer PS. This rather unexpected experimental observation was explained by using the thermodynamic argument that the effective Flory interaction parameter between the block copolymer K1102 and homopolymer PαMS is smaller than that between the block copolymer K1102 and homopolymer PS. In the absence of a rigorous theory which could enable one to predict the effective Flory interaction parameter for the *block* copolymer and homopolymer pair, we used the currently held mean-field theories.[46–48] We recommend that a statistical mechanical theory be developed for predicting the effective Flory interaction parameter for the block copolymer and homopolymer pair, which can take into account the local composition fluctuations.

To help interpret experimental results for the dynamic viscoelastic behavior of K1102/PαMS mixtures, we constructed phase diagrams using the experimental results of dynamic viscoelastic measurements and turbidity measurements. Experimental phase diagrams were compared

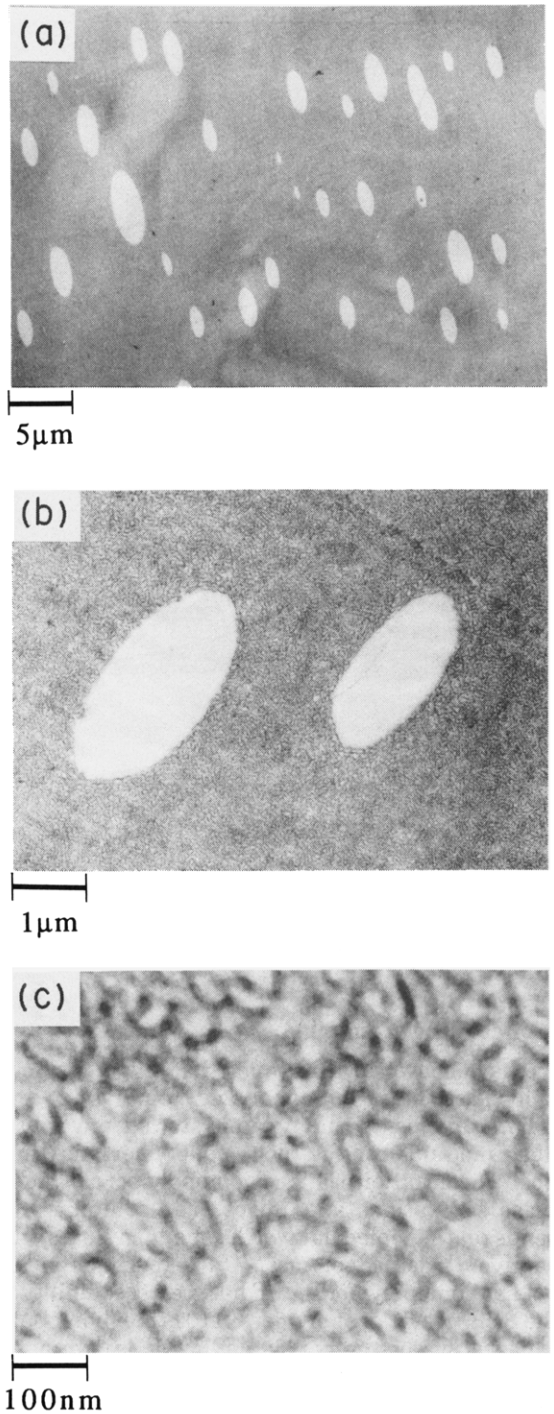

Figure 24. Transmission electron micrographs obtained on ultrathin sections stained by osmium tetroxide for the 50/50 K1102/PαMS8 mixture: (a) low magnification, (b) intermediate magnification, and (c) high magnification, showing the morphologies at 25 °C.

with theoretically predicted phase diagrams, which were obtained using the theory of Hong and Noolandi.[21] We have pointed out a direction for further theoretical development to improve upon the currently held theories. However, we wish to mention that the accuracy of the theoretical predictions presented in this paper is very sensitive to the accuracy of the interaction parameter used. In the present study we used the expressions for the interaction energy density Λ given in Table III, which were obtained from cloud point measurements and then curve-fitting the data to the Flory–Huggins theory. Recently, using experimental results from SAXS and the random phase approximation (RPA) method, Hashimoto and co-workers[14,60] investigated, in addition to the effect of temperature, the effect of the molecular weight of added homopolymer PS on the Flory–Huggins interaction parameter χ in mixtures of an SI diblock copolymer and a homopolymer PS and concluded that (a) as low molecular weight homopolymer PS was added, the values of χ increased, and (b) the values of χ depended on the degree of polymerization of the block copolymer. A series of recent papers by Freed and co-workers[61-63] caution, however, that the values of χ obtained from RPA calculation may not be accurate, since the RPA method is based on the assumption of incompressibility, which may not be valid for polymer blends and block copolymer melts. Note that in the use of the Flory–Huggins theory, the value of χ is independent of molecular weight.

Also, in this study, the morphological transition of ordered microdomains in the block copolymer K1102, as affected by the addition of homopolymer PαMS, was investigated using SAXS and TEM. Both SAXS and TEM provided very valuable information that could not be produced by the dynamic viscoelastic measurements and phase diagrams. Since the morphology (e.g., spheres, cylinders, or lamellae) of ordered microdomains in mixtures of a block copolymer and a homopolymer is believed to control their ultimate mechanical properties (e.g., shear adhesion, peel strength, and adhesive bond strength), we recommend that the morphology of ordered microdomains, together with dynamic viscoelastic properties, be investigated when developing formulas, for instance, for pressure-sensitive and hot-melt adhesives.[8-10,64]

References and Notes

(1) Present address: Department of Chemical Engineering, Sung Kyun Kwan University, Seoul, Korea.
(2) Burke, J. J.; Weiss, V., Eds. *Block and Graft Copolymers*; Syracuse University Press: Syracuse, NY, 1973.
(3) Ceresa, R. J., Ed. *Block and Graft Copolymerization*; Wiley: New York, 1973.
(4) Kraus, G.; Jones, F. B.; Marrs, O. L.; Rollmann, K. W. *J. Adhes.* **1977**, *8*, 235.
(5) Kraus, G.; Rollmann, K. W.; Gray, R. A. *J. Adhes.* **1979**, *10*, 221.
(6) Class, J. B.; Chu, S. G. *J. Appl. Polym. Sci.* **1985**, *30*, 805, 815, 825.
(7) Sheriff, M.; Knibbs, R. W.; Langely, P. G. *J. Appl. Polym. Sci.* **1973**, *17*, 3423.
(8) Kim, J.; Han, C. D.; Chu, S. G. *J. Polym. Sci., Part B: Polym. Phys.* **1988**, *26*, 677.
(9) Han, C. D.; Kim, J.; Baek, D. M. *J. Adhes.* **1989**, *28*, 201.
(10) Han, C. D.; Kim, J.; Baek, D. M.; Chu, S. G. *J. Polym. Sci., Part B: Polym. Phys.* **1990**, *28*, 315.
(11) Toy, L.; Ninomi, M.; Shen, M. *J. Macromol. Sci., Phys.* **1975**, *B11* (3), 281.
(12) Ninomi, M.; Akovali, G.; Shen, M. *J. Macromol. Sci., Phys.* **1977**, *B13* (1), 133.
(13) Zin, W. C.; Roe, R. J. *Macromolecules* **1984**, *17*, 183.
(14) Hashimoto, T.; Tanaka, H.; Hasegawa, H. In *Molecular Conformation and Dynamics of Macromolecules in Condensed Systems*; Nagasawa, M., Ed., Elsevier: Amsterdam, 1988; p 257.
(15) Hashimoto, T.; Tanaka, H.; Hasegawa, H. *Macromolecules* **1990**, *23*, 4378.
(16) Tanaka, H.; Hasegawa, H.; Hashmoto, T. *Macromolecules* **1991**, *24*, 240.
(17) Roe, R. J.; Zin, W. C. *Macromolecules* **1984**, *17*, 189.
(18) Nojima, S.; Roe, R. J. *Macromolecules* **1987**, *20*, 1866.
(19) Leibler, L.; Benoit, H. *Polymer* **1981**, *22*, 195.
(20) Benoit, H.; Wu, H.; Benmouna, M.; Mozer, B.; Bauer, B.; Lapp, A. *Macromolecules* **1985**, *18*, 986.
(21) Hong, K. M.; Noolandi, J. *Macromolecules* **1983**, *16*, 1083.
(22) Whitmore, M. D.; Noolandi, J. *Macromolecules* **1985**, *18*, 2486.
(23) In a previous study, Han and co-workers[32] used the block molecular weights, 10000S–50000B–50000S, as supplied by the manufacturer.
(24) Fetters, L. J. *J. Res. Natl. Bur. Stand.* **1966**, *70A*, 421.
(25) (a) Hashimoto, T.; Suehiro, S.; Shibayama, M.; Saijo, K.; Kawai, H. *Polym. J.* **1981**, *13*, 501. (b) Suehiro, S.; Saijo, K.; Ohta, Y.; Hashimoto, T.; Kawai, H. *Anal. Chim. Acta* **1986**, *189*, 41.

(26) Fujimura, M.; Hashimoto, T.; Kawai, H. *Mem. Fac. Eng. Kyoto Univ.* **1981**, *43*, 224.
(27) Hendricks, R. W. *J. Appl. Crystallogr.* **1972**, *5*, 315.
(28) Krause, S.; Lu, Z.; Iskandar, M. *Macromolecules* **1982**, *15*, 1076.
(29) There is experimental evidence[28] suggesting that the T_g of the PS endblock in an SB or SBS block copolymer is lower by about 18 °C than that of homopolymer PS with identical molecular weight. A similar observation was also reported for SI diblock copolymer by: Morese-Seguela, B.; St-Jacques, M.; Renaud, J. M.; Prud'homme, J. *Macromolecules* **1980**, *13*, 100.
(30) This trend can also be confirmed by SAXS invariant analysis.
(31) Fox, T. G. *Bull. Am. Phys. Soc.* **1956**, *1*, 126.
(32) Han, C. D.; Kim, J.; Kim, J. K. *Macromolecules* **1989**, *22*, 383.
(33) Han, C. D.; Kim, J. *J. Polym. Sci., Part B: Polym. Phys.* **1987**, *25*, 1741.
(34) Han, C. D.; Baek, D. M.; Kim, J. K. *Macromolecules* **1990**, *23*, 561.
(35) Hashimoto, T.; Koizumi, S.; Hasegawa, H.; Izumitani, T.; Hyde, S. T. *Macromolecules* **1992**, *25*, 1433.
(36) Zin, W. C.; Roe, R. J. *Macromolecules* **1980**, *13*, 1221.
(37) Lin, J. L.; Roe, R. J. *Macromolecules* **1987**, *20*, 2168.
(38) Richardson, M. J.; Savill, N. G. *Polymer* **1977**, *18*, 3.
(39) Rigby, D.; Roe, R. J. *Macromolecules* **1986**, *19*, 721.
(40) Cowie, J. M. G.; Toporowski, P. M. *J. Macromol. Sci., Phys.* **1969**, *B3*, 81.
(41) Leibler, L. *Macromolecules* **1980**, *13*, 1602.
(42) Fredrickson, G. H.; Helfand, E. *J. Chem. Phys.* **1987**, *81*, 697.
(43) Burger, C.; Ruland, W.; Semenov, A. N. *Macromolecules* **1990**, *23*, 3339.
(44) Helfand, E.; Wasserman, Z. *Macromolecules* **1976**, *9*, 879; **1978**, *11*, 960; **1980**, *13*, 994; In *Development in Block Copolymers*; Goodman, I., Ed.; Applied Science: New York, 1982; Chapter 4.
(45) Previously, using the block molecular weights, 10000S–50000B–10000S, for K1102 Han and co-workers obtained T_r = 213 °C.[32]
(46) Kambour, R. P.; Bendler, J. T.; Bopp, R. C. *Macromolecules* **1983**, *16*, 753.
(47) ten Brinke, G.; Karasz, F. E.; MacKnight, W. J. *Macromolecules* **1983**, *16*, 1827.
(48) Paul, D. R.; Barlow, J. W. *Polymer* **1984**, *25*, 487.
(49) Ijichi, Y.; Hashimoto, T. *Polym. Commun.* **1988**, *29*, 135.
(50) Tanaka, H.; Hashimoto, T. *Polym. Commun.* **1988**, *29*, 212.
(51) Inoue, T.; Soen, T.; Hashimoto, T.; Kawai, H. *J. Polym. Sci., Part A-2* **1969**, *7*, 1283.
(52) Uchida, T.; Soen, T.; Inoue, T.; Kawai, H. *J. Polym. Sci., Part A-2* **1972**, *10*, 101.
(53) Keller, A.; Pedemonte, E.; Willmouth, F. M. *Kolloid Z., Z. Polym.* **1970**, *238*, 385.
(54) Gallot, R. B. *Adv. Polym. Sci.* **1978**, *29*, 85.
(55) Meier, D. J. *Polym. Prepr. (Am. Chem. Soc., Div. Polym. Chem.)* **1970**, *11*, 400.
(56) Ohta, T.; Kawasaki, K. *Macromolecules* **1986**, *19*, 2621.
(57) Hasegawa, H.; Tanaka, H.; Yamasaki, K.; Hashimoto, T. *Macromolecules* **1987**, *20*, 1651.
(58) Koizumi, S.; Hasegawa, H.; Hashimoto, T., in preparation.
(59) Molau, G. E. In *Block Copolymers*; Aggarwal, S. L., Ed.; Plenum Press: New York, 1970; p 79.
(60) Tanaka, H.; Hashimoto, T. *Macromolecules* **1991**, *24*, 5398.
(61) McMullen, W. E.; Freed, K. F. *Macromolecules* **1990**, *23*, 255.
(62) Dudowicz, J.; Freed, K. F. *Macromolecules* **1990**, *23*, 1519.
(63) Tang, H.; Freed, K. F. *Macromolecules* **1991**, *24*, 958.
(64) Kraus, G.; Hashimoto, T. *J. Appl. Polym. Sci.* **1982**, *27*, 1745.

Registry No. PαMS, 25014-31-7; PS, 9003-53-6.